

1 Estimation of mechanistic parameters in the gas-phase reactions of 2 ozone with alkenes for use in automated mechanism construction

3 Mike J. Newland^{1,a}, Camille Mouchel-Vallon^{1,b}, Richard Valorso², Bernard Aumont², Luc
4 Vereecken³, Michael E. Jenkin⁴, Andrew R. Rickard^{1,5}

5 ¹ Wolfson Atmospheric Chemistry Laboratories, Department of Chemistry, University of York, United Kingdom

6 ² Univ Paris Est Creteil and Université de Paris, CNRS, LISA, F-94010 Créteil, France.

7 ³ Forschungszentrum Jülich GmbH, Institute for Energy and Climate, IEK-8 Troposphere, 52428 Jülich, Germany

8 ⁴ Atmospheric Chemistry Services, Okhampton, Devon, EX20 4QB, United Kingdom.

9 ⁵ National Centre for Atmospheric Science, Wolfson Atmospheric Chemistry Laboratories, University of York,
10 United Kingdom.

11
12 ^a now at: ICARE-CNRS, 1 C Av. de la Recherche Scientifique, 45071 Orléans Cedex 2, France.

13 ^b now at: Laboratoire d'Aérodynamique, Université de Toulouse, CNRS, UPS, Toulouse, France.

14 Correspondence to: Mike Newland (mike.newland@gmail.com) and Andrew Rickard
15 (andrew.rickard@york.ac.uk).

16

17 **Abstract.** Reaction with ozone is an important atmospheric removal process for alkenes. The ozonolysis reaction
18 produces carbonyls, and carbonyl oxides (Criegee intermediates, CI), which can rapidly decompose to yield a
19 range of closed shell and radical products, including OH radicals. Consequently, it is essential to accurately
20 represent the complex chemistry of Criegee intermediates in atmospheric models in order to fully understand the
21 impact of alkene ozonolysis on atmospheric composition. A mechanism construction protocol is presented which
22 is suitable for use in automatic mechanism generation. The protocol defines the critical parameters for describing
23 the chemistry following the initial reaction, namely: the primary carbonyl / CI yields from the primary ozonide
24 fragmentation; the amount of stabilisation of the excited CI; the unimolecular decomposition pathways, rates and
25 products of the CI; the bimolecular rates and products of atmospherically important reactions of the stabilised CI
26 (SCI). This analysis implicitly predicts the yield of OH from the alkene-ozone reaction. A comprehensive database
27 of experimental OH, SCI and carbonyl yields has been collated using reported values in the literature and used to
28 assess the reliability of the protocol. The protocol provides estimates OH, SCI and carbonyl yields with a root
29 mean square error of 0.13 and 0.12 and 0.14, respectively. Areas where new experimental and theoretical data
30 would improve the protocol and its assessment are identified and discussed.

Deleted: (CI*)

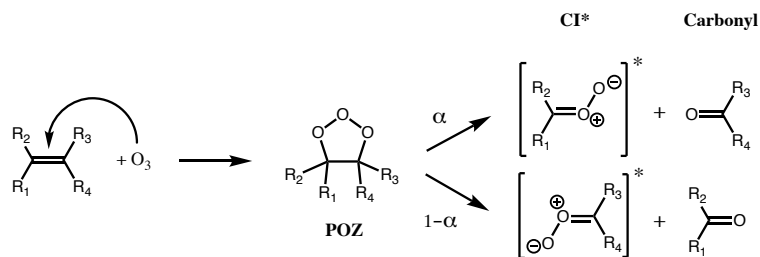
31 1 Introduction

32 Reaction with ozone is an important atmospheric removal process for alkenes, competing with reaction with OH
33 and NO₃ radicals. The ozonolysis reaction produces carbonyls and carbonyl oxides, commonly denoted Criegee
34 intermediates (CI), which can rapidly rearrange or decompose to yield a range of closed shell and radical products
35 (Johnson and Marston, 2008). Alkene ozonolysis has been shown to be an important non-photolytic source of OH
36 radicals, with field measurements (Paulson and Orlando, 1996; Elshorbany et al., 2009) and modelling studies
37 (e.g. Bey et al., 1997) suggesting it to be the dominant tropospheric OH source at night, in the winter (Heard et
38 al., 2004; Emmerson et al., 2005), and in indoor environments (Carslaw, 2007). Unimolecular CI reactions (Ehn
39 et al. 2014; Iyer et al., 2020) and bimolecular reactions of Stabilised Criegee Intermediates (SCI), with e.g. organic
40 acids and peroxy radicals (e.g. Kristensen et al., 2014; Sakamoto et al., 2013; Zhao et al., 2015; Mackenzie-Rae

et al., 2016), have been implicated in secondary organic aerosol formation. SCI can also act as an oxidant, this has been studied particularly for the reaction with SO₂ (e.g. Welz et al., 2012, Mauldin et al., 2012; Caravan et al., 2020) which can lead to sulfate aerosol production and hence impact radiative forcing and climate (Pierce et al. 2013; Percival et al. 2013). However, both the SO₂ and organic acid reactions, while important locally, are likely only of minor importance to global budgets of sulfate aerosol and organic acids (Welz et al., 2014; Newland et al., 2018). The dominant removal processes for most SCI in the troposphere are reaction with water vapour or unimolecular reaction (Vereecken et al., 2017). However, for certain structures, these reactions are sufficiently slow for bimolecular reactions with other trace gases to become important.

Understanding of the complex nature of the chemistry of Criegee intermediates has progressed rapidly in recent years, particularly with regard to the mechanisms and rates of decomposition of CI (i.e. SCI and chemically excited CI (CI*)), and the bimolecular reaction rates of SCI. This has been facilitated by: direct experimental measurements of CI kinetics, generating CI through photolysis of di-iodo precursors (e.g. Welz et al., 2012; Chhantyal-Pun et al. 2020, and references therein); indirect measurements of CI kinetics during alkene ozonolysis experiments (e.g. Berndt et al. 2014a, 2014b, 2015; Newland et al., 2015), and extensive theoretical studies (e.g. Vereecken et al., 2017, and references therein).

The reaction of ozone with alkenes proceeds by a concerted addition to the C=C double bond, forming a short lived Primary Ozonide (POZ). Typically, the POZ fragments into two pairs of carbonyls and Criegee intermediates (CI) (Figure 1); for small to medium sized alkenes (C_{≤10}) this POZ is vibrationally excited, decomposing promptly, while for large alkenes (e.g. C_{≥15}, sesquiterpenes), theoretical studies suggest that the POZ can be collisionally stabilized prior to decomposition (Chuong et al., 2004; Nguyen et al., 2009a). Theoretical work also indicates that a small fraction of the POZ can rearrange to a carbonyl-hydroperoxide when vinylic H-atoms are present (Pfeifle et al., 2018); this mechanism is discussed separately below. It has also been suggested that different pathways may play a more significant role for a small number of systems e.g. cyclohexadienes (Pinelo et al., 2013).



66
67

68 **Figure 1. First step of alkene ozonolysis. A primary ozonide (POZ) is formed which rapidly decomposes to yield a pair**
69 **of chemically activated Criegee intermediates and carbonyl products.**

70 Criegee intermediates are generally zwitterionic in nature, as shown in Figure 1, but the moiety is denoted
71 simply as a >COO structure below (not to be confused with alkylperoxy radicals, ROO[•]). CI can be formed with
72 the terminal oxygen of the carbonyl oxide moiety in either an *E* (*anti*) or *Z* (*syn*) configuration relative to a given
73 substituent group. The two conformers are not in rapid equilibrium, with quantum calculations showing that the
74 energy barrier to rotational interconversion for CH₃CHO is about 210 kJ mol⁻¹ (Johnson and Marston, 2008, and
75 references therein); this was confirmed by Vereecken et al. (2017) who calculated barriers exceeding 120 kJ mol⁻¹

Deleted: II

Deleted: */SCI

Deleted: 29 kcal

Deleted: 30 kcal

80 ¹ for saturated CI conformers. Isomeric CI conformers have been shown to have different unimolecular reaction
81 rates (e.g. Vereecken et al., 2017), follow different unimolecular pathways (Herron and Huie, 1977; Niki et al.,
82 1987; Martinez and Herron, 1987; Kidwell et al., 2016), and have very different reaction rates with water (e.g.
83 Taatjes et al., 2013; Sheps et al., 2014; Huang et al., 2015). Therefore, these conformers must necessarily be
84 considered as separate species, irreversibly partitioned according to their nascent ratios, to accurately represent
85 the effects of alkene ozonolysis on atmospheric composition.

86 Structure Activity Relationships (SARs) are commonly used to design the protocols needed to develop
87 automated mechanism generation tools (Vereecken et al., 2018). This paper forms part of a series of articles
88 devoted to the development of SARs for mechanism generation (Jenkin et al., 2018a, 2018b, 2019, 2020). Updated
89 SAR methods for the initial reactions of O₃ with unsaturated organic compounds are presented in a companion
90 paper (Jenkin et al., 2020), while in this work, a protocol is presented for the subsequent chemistry occurring
91 following the initial O₃ addition. This [protocol](#) details the yields of carbonyls and Criegee intermediates from the
92 alkene + O₃ reaction, and the subsequent fate of the Criegee intermediates, and accounts for the minor pathway
93 by carbonyl-hydroperoxide radical formation. The protocol is based on available experimental data and theoretical
94 data combined. For areas in which limited data exists, the protocol is set up to be easily updated as new
95 experimental or theoretical results become available. These areas are highlighted in the paper and are
96 recommended areas of further research. The protocol is currently being used to guide development of alkene
97 ozonolysis chemistry in the Generator for Explicit Chemistry and Kinetics of Organics in the Atmosphere,
98 GECKO-A (Aumont et al., 2005), and the Master Chemical Mechanism, MCM (Jenkin et al., 1997, Saunders et
99 al., 2003). It is noted that the protocol does not currently consider aromatic species that have been shown to react
100 with ozone, such as catechols, for which the mechanism may be different to the Criegee mechanism described
101 here.

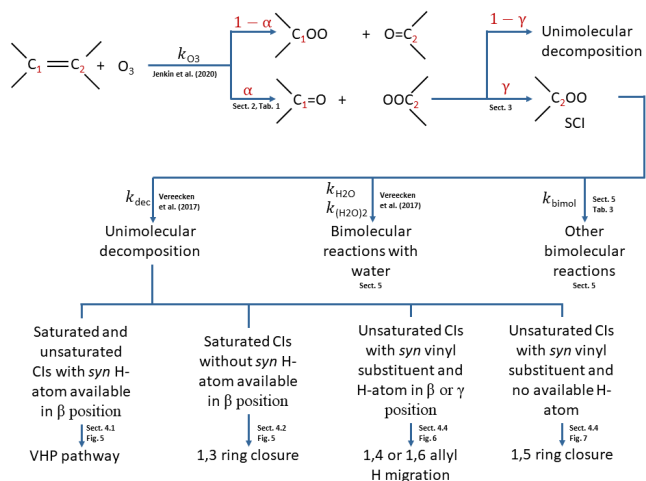
102 The methodology for applying the protocol described in this work is summarised in [Figure 2](#). The initial
103 addition of ozone to the double bond follows the protocol described in the companion paper (Jenkin et al., 2020).
104 The POZ formed from this protocol then decomposes according to the rules determined in Section 2, to give the
105 primary carbonyl and the CI yields (α), and possibly a minor fraction of carbonyl-hydroperoxide. A fraction (γ)
106 of the CI is then stabilised (Section 3). Both the stabilised and chemically activated CI then follow the relevant
107 set of rules from Vereecken et al. (2017) to ascribe them unimolecular decomposition mechanisms (and hence
108 products) and rates (Section 4), and bimolecular reaction rates with water vapour (Section 5). Finally, bimolecular
109 reaction rates with other atmospherically important species are assigned as a function of the SCI structure (Section
110 5).
111

Formatted: Font: (Default) +Headings CS (Times New Roman), 10 pt, Not Bold

Deleted: Figure 2

Formatted: Font: (Default) +Headings CS (Times New Roman), 10 pt

Formatted: Font: (Default) +Headings CS (Times New Roman), 10 pt, Not Bold, Not Italic



113

114 **Figure 2. Flow diagram for implementation of the protocol. α = branching ratios in POZ decomposition, γ = fraction of**
 115 **CI stabilised. >COO denotes the Criegee intermediate formed.**

116 2 Primary Ozonide Fragmentation

117 2.1 Alkenes with aliphatic substituents

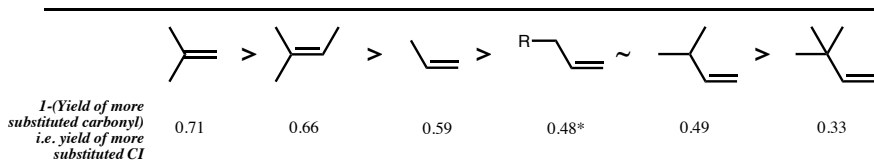
118 The fragmentation of the POZ has previously been parameterized based on the branching pattern around the
 119 double bond of the parent alkene (Jenkin et al., 1997; Rickard et al., 1999). Generally, it can be said that there is
 120 a preference for formation of the more substituted CI, e.g. the ozonolysis of 2-methyl propene yields ~0.7
 121 $(\text{CH}_3)_2\text{COO}$ and ~0.3 CH_2OO (Rickard et al., 1999). However, consideration of just the immediate substituents
 122 of the double bond breaks down for more complex structures and for oxygenated substituents. There is clearly
 123 also an effect of substitution around the carbon adjacent to the double bond (the α -carbon atom). For instance,
 124 when there is a *t*-butyl group attached to the double bond, a strong preference is seen for formation of the opposing
 125 CI, as observed for yields of trimethylacetaldehyde from 3,3-dimethyl-1-butene (0.67) and trans-2,2-dimethyl-3-
 126 hexene (0.84) (Grosjean and Grosjean, 1997a). Using data from Grosjean and Grosjean (1997a), various
 127 homologous series of alkenes can be considered, such as the series with increasing methyl substitution on the α -
 128 carbon. For the 1-alkene series (Figure 3), yields of the larger carbonyl of 0.35, 0.51, and 0.67 are determined for
 129 1-butene, 3-methyl-1-butene, 3,3-dimethyl-1-butene respectively.

130

Formatted: Font: 10 pt, Not Bold, Font colour: Black

Formatted: Font: 10 pt, Not Bold, Not Italic, Font colour: Black

Deleted: Figure 3



132
133 **Figure 3. Decreasing order of preference, from left to right, of more substituted CI formation from ozonolysis of**
134 **example alkyl substituted alkenes. Values are 1 – (mean of measured yields of carbonyls) (Spreadsheet S1). * Mean**
135 **measured yield of propanal (i.e. 1 – more substituted CI) formation from 1-butene is 0.35, but for all other 1-alkenes**
136 **the yield of the larger primary carbonyl product ranges from 0.45 – 0.50.**

137 Such relationships have been observed and discussed previously by Grosjean and Grosjean (1997a) in terms of:
138 (i) steric hindrance potentially weakening the O-O bond in the POZ on the side of the bulky substituent, and (ii)
139 the inductive effect of adjacent alkyl groups strengthening the O-O bonds in the POZ (Grosjean and Grosjean,
140 1997a). Earlier work considering POZ fragmentation in the aqueous phase (Fliszár and Renard, 1970; Fliszár and
141 Granger, 1970; Fliszár et al., 1971) described similar relationships to those observed in the gas phase (i.e. that
142 shown in [Figure 3](#)), except in the case of terminal alkenes, for which the reverse trend was observed. In these
143 studies, the observed trends are discussed in terms of stabilisation of the positive charge on the carbon in the POZ
144 through: (i) ‘hyperconjugative stabilisation’ in the transition state, and (ii) the inductive effect during the POZ
145 cleavage, with steric effects discounted as being unimportant in determining the POZ fragmentation pattern.

146 [Finally, Vereecken et al. \(2017, Table 16 in the supplementary material\) analyse the stability of CI in terms of](#)
147 [group additivity factors, showing that alkyl-substituted CI are more stable than H-substituted CI, but where the](#)
148 [stability of the CI is inversely proportional to the branching on the β-carbon atom](#)

149 These works can be summarised by saying that it appears that a substituent with a partial negative charge,
150 such as a methyl group, can stabilise the positive charge on the adjacent carbon in the POZ. This leads to a greater
151 yield of the CI containing the more stabilising substituents. On the other hand, a substituent that leads to a partial
152 positive charge on the α-carbon leads to a lower yield of that CI.

153 2.2 Oxygenated alkenes

154 Following the rationale discussed above, oxygenated substituents on the α-carbon might be expected to strongly
155 influence the primary ozonide fragmentation pattern. The number of product yield studies on the ozonolysis of
156 most classes of unsaturated oxygenates is rather limited. As discussed below, some oxygenated substituents appear
157 to destabilise the positive charge on the carbon in the POZ (i.e. disadvantaging POZ fragmentation towards the
158 production of the CI on the oxygenated side), particularly carbonyl groups, while others such as acrylate esters
159 and carboxylic acids may stabilise the CI, favouring its formation. However, data is very limited and often
160 ambiguous for most of the oxygenated classes. This is partly due to challenges in measuring products containing
161 multiple oxygenated groups, partly that some of these classes are likely to be present in negligible amounts in the
162 atmosphere and, for some, that ozonolysis will be a negligible atmospheric sink compared to e.g. reaction with
163 OH or photolysis. The available data is provided in the Supplement, Spreadsheet S1.

164 2.2.1 Enones / enals

165 Primary carbonyl yields have been reported for two α-β terminally unsaturated ketones (H₂C=CHC(O)R). For
166 methyl vinyl ketone (MVK), Grosjean et al. (1993) and Ren et al. (2017) determined a strong preference for

Deleted: 64

Deleted: are

Deleted: Figure 3

Formatted: Font: (Default) +Headings CS (Times New Roman), 10 pt, Not Bold, Font colour: Black

170 formation of the ketone substituted product methyl glyoxal (0.87 and 0.71 ± 0.06 (with no OH scavenger)
171 respectively). For ethyl vinyl ketone, primary carbonyl yields for formaldehyde (HCHO) and 2-oxobutanal have
172 been determined to be 0.55 and 0.44 (Grosjean et al., 1996), and 0.37 and 0.49 (Kalalian et al., 2020) respectively,
173 displaying no clear preference for either fragmentation pathway. For α - β unsaturated ketones ($R_1CH=CHC(O)R_2$),
174 Grosjean and Grosjean (1999) measured the primary carbonyl yields from ozonolysis of 4-hexen-3-one to be:
175 acetaldehyde (CH_3CHO), 0.51 ± 0.01 , and 2-oxobutanal ($CH_3CH_2C(O)CHO$), 0.56 ± 0.02 , while Wang et al. (2015)
176 measured the primary carbonyl yields from ozonolysis of 3-methyl-3-buten-2-one ($CH_2=CR_1C(O)R_2$) to be:
177 diacetyl ($CH_3COCOCH_3$) 0.30 ± 0.03 , and HCHO 0.44 ± 0.05 , and from 3-methyl-3-penten-2-one
178 ($R_1CH=CR_2C(O)R_3$), diacetyl 0.39 ± 0.04 and CH_3CHO 0.61 ± 0.07 . For ozonolysis of 2-enals, yields have been
179 reported for crotonaldehyde (2-butenal) (CH_3CHO 0.42, glyoxal 0.47) (Grosjean and Grosjean, 1997b) and trans-
180 2-hexenal (butanal 0.53, glyoxal 0.56) (Grosjean et al., 1996). For the atmospherically important isoprene
181 oxidation product methacrolein (2-methyl-prop-2-enal, MACR), Grosjean et al. (1993) measured yields of methyl
182 glyoxal of 0.58 ± 0.06 and HCHO of 0.12 ± 0.03 . For 2-ethyl acrolein, the ethyl glyoxal yield has been measured to
183 be 0.14 by Grosjean et al. (1994), and 0.49 ± 0.03 by O'Dwyer et al. (2010).

184 To summarise, the presence of a carbonyl group on a double bond appears to favour formation of the
185 opposing CI. However, this effect is neutralised to an extent by the presence of an alkyl substituent on the same
186 side of the double bond, e.g. in the case of 3-methyl-3-buten-2-one, methacrolein, and 2-ethyl acrolein. There
187 remain large uncertainties on the trends in these classes (it is noted that in some cases the sum of the measured
188 primary carbonyl yields is well below one). They clearly warrant further study, owing to the significance of these
189 classes of compounds in atmospheric chemistry (e.g. MACR and MVK from isoprene oxidation (Wennberg et al.,
190 2018)).

191 2.2.2 Enols / enol ethers

192 There has been very little experimental work on the atmospheric chemistry of enols due to difficulties in synthesis,
193 storage, and measurement of these compounds. However, two recent theoretical studies examined the ozonolysis
194 of enols. The first (Lei et al., 2020) on the simplest enol, vinyl alcohol (ethenol), suggested that formation of
195 $CH_2OO + HCOOH$ is strongly favoured (~78 %). The second (Wang et al., 2020), on the complex ketene-enol
196 species 4-hydroxy-1,3-butadien-1-one, also suggests that formation of HCOOH and the corresponding CI is
197 strongly favoured (84 %). By contrast, there have been several experimental studies on the product yields of the
198 reactions of enol ethers ($R_1-O-CR_2=CR_3R_4$) with ozone. Most studies (Thiault et al., 2002; Klotz et al., 2004;
199 Barnes et al., 2005; Zhou et al., 2006; Zhou, 2007; Al Mulla et al., 2010) have determined that the dominant POZ
200 decomposition channel yields the formate ($R_1-O-C(O)R_2$) and the corresponding CI (R_3R_4COO), with measured
201 yields of the formate ranging from 55 % - 89 % (see Spreadsheet S1). An exception to these studies is the work
202 of Grosjean and Grosjean (1997b; 1999), which tended to find similar yields of the two primary carbonyl products.

203 2.2.3 Esters / acids

204 The primary carbonyl products of ozonolysis of the acrylate esters: methyl acrylate, ethyl acrylate, and methyl
205 methacrylate were studied by Bernard et al. (2010). Grosjean and Grosjean (1997b) also studied methyl acrylate.
206 There is no clear evidence for a preferential route for POZ fragmentation in these studies (see Spreadsheet S1).
207 The primary carbonyl yields from vinyl acetate ozonolysis were measured to be 0.30 ± 0.04 and 0.70 ± 0.08 for

Deleted: of

209 HCHO and CH₃C(O)OC(O)H respectively by Al Mulla et al. (2010), and 0.20±0.06 and 0.97±0.08 by Picquet-
210 Varrault et al. (2010). These studies suggest a preference for formation of CH₂OO and the anhydride. There are
211 only two compounds reported for ozonolysis of α-β unsaturated acids: acrylic and methacrylic acid. For acrylic
212 acid ozonolysis in the presence of formic acid as an SCI scavenger, Al Mulla et al. (2010) measured yields of 1.48
213 ± 0.2 and < 0.1 for HCHO and HC(O)C(O)OH respectively, while in the absence of formic acid that group
214 measured a yield of HCHO of 0.95 (Viero, 2008). For methacrylic acid, Al Mulla et al. (2010) measured yields
215 of 0.77 ±0.07 and 0.74 ±0.10 for HCHO and CH₃C(O)C(O)OH respectively. It is difficult to rationalise these
216 results: the acrylic acid experiments suggest a preference for formation of the CI with the acid moiety, but the
217 methacrylic acid experiments suggest that the presence of a methyl group on the same side of the double bond as
218 the acid reduces this preference, in contrast to most other systems where methyl substitution increases the yield
219 of that CI. This is a recommended area for further study.

Deleted: acetate

220 2.2.4 Alcohols

221 There are significant differences between measured primary carbonyl yields from the ozonolysis of α,β-
222 unsaturated acyclic alcohols between studies by Grosjean and Grosjean (1997b), Le Person et al. (2009), O'Dwyer
223 et al. (2010) and Kalalian et al. (2020). This is likely owing to different experimental setups between groups, and
224 the difficulty of quantitatively measuring compounds with multiple oxygenated substituents. Overall the data in
225 Spreadsheet S1 suggest that the presence of a hydroxyl group in place of a hydrogen on the α-carbon may lead to
226 a slight preference for CI production on the other side of the double bond to the hydroxyl group.

227 2.3 Conjugated alkenes

228 The ozonolysis of conjugated alkenes leads to POZ with a vinyl substituent on the α-carbon. For non-symmetrical
229 conjugated alkenes, the measurement of primary carbonyl yields can only be used to determine the POZ
230 fragmentation if the relative contribution of reaction at each double bond to the overall reaction rate is known. For
231 ozonolysis of the atmospherically important biogenic alkene isoprene, the primary carbonyl yields recommended
232 by IUPAC (Atkinson et al., 2006; iupac-aeris.ipsl.fr, last accessed 6 December 2021) are: methyl vinyl ketone
233 (MVK), 0.17; methacrolein (MACR), 0.41; and HCHO 0.42. Based on reported product yields, the contribution
234 of reaction to each double bond to the overall rate has been estimated to be 0.6 for the terminal double bond and
235 0.4 for the substituted double bond (Nguyen et al., 2016; Jenkin et al., 2020). However, to the authors' knowledge
236 there has been no direct measurement of the reaction at each double bond, and this represents a significant
237 uncertainty in one of the most important atmospheric ozonolysis systems. Based on this assumption, and the
238 recommended yields of MVK and MACR, the formation of MACR+CH₂OO is favoured over methacrolein oxide
239 (MACRO) + HCHO, and there is a slight preference for formation of methyl vinyl ketone oxide (MVKO) +
240 HCHO compared to MVK+CH₂OO. The MACR channel would suggest that the vinyl substituent is less
241 favourable in the POZ decomposition, compared to a hydrogen. The methyl group present in MVKO stabilises the
242 CI (see section 2.1), leading to a preference for this channel. For symmetrical alkenes, the primary carbonyl yields
243 should be directly representative of the POZ fragmentation. For 1,3-butadiene, an acrolein yield of 51 – 52 % has
244 been measured (Niki et al., 1983; Kramp and Paulson, 2000), suggesting little preference for either POZ
245 decomposition pathway, in contrast to the analogous MACR channel in isoprene. Lewin et al. (2001) reported
246 complementary carbonyl yields from ozonolysis at the internal bond of (*E*) and (*Z*)-penta-1,3-diene and 5-

Deleted: destabilising

249 methylhexa-1,3-diene, which all showed a preference for formation of the unsaturated carbonyl (i.e. the saturated
250 CI), suggesting that the vinyl group is less favourable than a methyl or isopropyl group, in agreement with the
251 observations from isoprene. Note that, once the unsaturated CI is formed, the vinyl group can conjugate with the
252 carbonyl oxide π -system, leading to additional stabilization such that vinyl-CI are more stable than H-substituted
253 CI (Vereecken et al. 2017); this is however a product-specific effect that is not available yet in the POZ
254 decomposition.

Deleted: stabilising

255 2.4 Endocyclic alkenes

256 Decomposition of the POZ formed in the ozonolysis of endocyclic alkenes, leads to a molecule containing both
257 the carbonyl oxide and carbonyl moieties. Thus for non-substituted cycloalkenes (e.g. cyclopentene) there is only
258 one possible CI that can be formed (which can be in either the *E* or *Z* configuration). This means that there are no
259 stable primary carbonyls formed and so the relative contributions of the POZ decomposition pathways cannot be
260 inferred from measured primary carbonyl yields as they can for aliphatic compounds. Even a simple endocyclic
261 system such as cyclohexene gives a complex range of gas-phase (Aschmann et al., 2003; [Hansel et al., 2018](#)) and
262 aerosol phase (Kalberer et al., 2000; Ziemann, 2002) products, which can be attributed to decomposition of both
263 the *E* and *Z* forms of hexanal carbonyl oxide. However, the measured OH yields can be used to give an estimate
264 of the amount of CI decomposing via the vinyl-hydroperoxide (VHP) pathway (see section 4.1). It is noted here
265 that it has been proposed that alternative unimolecular pathways (that do not yield OH) are available to the CI
266 formed from endocyclic alkenes (Chuong et al., 2004; Nguyen et al., 2009a; Long et al., 2019), but that these are
267 only dominant for stabilised CI. Since the stabilised CI yield is low for endocyclic alkenes, at least up to C₁₀
268 (monoterpenes) (Chuong et al., 2004), measured OH yields should give a fair representation of the relative amount
269 of CI decomposing via the VHP pathway). For non-substituted cycloalkenes, OH yields have been compiled by
270 Calvert et al. (2000) covering cyclo-pentene, -hexene, -heptene, -octene and -decene from a number of research
271 groups (Spreadsheet S2). There is some spread in the data but no clear evidence for favouring formation of *E* or
272 *Z* CI, i.e. OH yields tend to centre around ~0.5. For substituted cycloalkenes, Atkinson et al. (1995) measured an
273 OH yield of 0.90 for 1-methyl-1-cyclohexene, suggesting either that the dominant CI formed is the di-substituted
274 CI (which will then undergo decomposition via the VHP pathway to yield OH), or that the mono-substituted CI
275 is formed predominantly as the *syn* conformer. The former must be considered more likely based on the observed
276 trends in aliphatic alkenes for favouring formation of the more substituted CI, and that there appears to be little
277 preference for formation of *syn/anti*-CI from non-substituted endocyclic alkenes. 1-methyl-1-cyclohexene is
278 particularly important from the point of view of atmospheric chemistry as an analogue for the abundant biogenic
279 monoterpenes α -pinene and limonene. OH yields from α -pinene and limonene ozonolysis have been measured
280 by a number of groups and are also generally high (0.64-0.91) (Cox et al. 2020), similar to 1-methyl-1-
281 cyclohexene.

282 2.5 Exocyclic alkenes

283 For exocyclic alkenes in which the double bond is attached to the ring, e.g. β -pinene, the data suggests that POZ
284 fragmentation strongly favours formation of the ring containing CI. For the monoterpene β -pinene, the mean
285 measured yield of the C₉ carbonyl, nopinone, is 0.21 (Grosjean et al., 1993; Hakola et al., 1994; Rickard et al.,
286 1999; Yu et al., 1999; Winterhalter et al., 2000; Hasson et al., 2001b; Lee et al., 2006; Ma and Marston, 2008),

288 with theoretical work (Nguyen et al., 2009b) suggesting that some of this may be secondary and that the primary
289 yield could be even lower. The other two compounds with a terminal double bond attached to the ring for which
290 there are data are camphene (0.36 yield of C₉ carbonyl (Hakola et al., 1994; Hasson et al., 2001b)) and methylene
291 cyclohexane (0.19 yield of C₆ carbonyl (Hasson et al., 2001b)). For the monoterpene sabinene, which has a
292 terminal double bond attached to a C₅ and C₇ ring, the mean measured yield of the C₉ carbonyl, sabinaketone, is
293 0.44. This is considerably higher than from those compounds where the double bond is on a C₆ ring, probably
294 demonstrating the impact of ring strain on the POZ fragmentation. The monoterpene terpinolene has a
295 disubstituted double bond attached to a six membered ring. Reported yields of the ring containing carbonyl
296 (0.40±0.06 (Hakola et al., 1994); 0.40±0.08 (Reissell et al., 1999); 0.45 (Ma and Marston, 2009)) suggest yields
297 of the ring containing CI of 0.60 and 0.55 respectively; this assumes 100% reaction at the exocyclic double bond,
298 with Hakola et al. (1994) measuring a yield of ≤ 2 % of the dicarbonyl expected as a product (though by no means
299 the only one) from reaction at the endocyclic double bond. These CI yields are lower than for the exocyclic alkenes
300 with terminal double bonds, but are still considerably higher than most compounds which have a dimethyl
301 substitution on the double bond, for which acetone yields tend to be ~ 0.3. The presence of a ring clearly has a
302 different effect to simply having two alkyl groups attached to the double bond, leading to much higher yields of
303 the ring containing CI.

304 For alkenes with a vinyl group attached to a ring, there are data only for vinyl cyclohexane, and its aromatic
305 analogue styrene. These have similar yields for the ring containing carbonyl of 0.62 and 0.64 respectively
306 (Grosjean and Grosjean, 1997a). There is no data for alkenes with double bonds more distant from a ring.

307 2.6 Yields of CI stereo-conformers

308 The formation of *syn/anti* conformers of CI in alkene ozonolysis was first discussed by Bauld et al. (1968), to
309 explain the observed *cis/trans* yields of the secondary ozonide formed from ozonolysis in the aqueous phase. Their
310 observations suggested that ozonolysis of *cis*-alkenes will predominantly form *anti*-CI, while for *trans*-alkenes
311 the predominance was less clear and appeared to be dependent on alkene structure. In the gas phase, but-2-ene is
312 the most studied system. Various experimental work has observed higher yields of OH from *trans*-but-2-ene
313 compared to *cis*-but-2-ene (see Spreadsheet S3). Assuming that only (*Z*)-CI decomposition yields OH (see Section
314 4.1), this implies a higher *nascent* (*Z*):(*E*)-CH₃CHOO ratio from decomposition of the POZ formed in *trans*-but-
315 2-ene ozonolysis. Orzechowska and Paulson (2002) measured a ratio of 1.62 for the OH yields from *trans/cis*-
316 but-2-ene. They observed a similar relationship for *trans/cis*-pent-2-ene and *trans/cis*-hex-3-ene, with OH yield
317 ratios determined as 1.80 and 1.51 respectively. Assuming that OH comes exclusively from (*Z*)-CH₃CHOO
318 implies a (*Z*):(*E*)-RCHOO ratio of 0.60:0.40 – 0.64:0.36 for these three systems. Kroll et al. (2002) determined a
319 similar OH yield ratio for *trans/cis*-hex-3-ene, but using isotopically labelled hydrogen atoms demonstrated that
320 a fraction of this OH was not coming from the (*Z*)-CI. From their OH yield measurements, they inferred a (*Z*):(*E*)-
321 C₂H₅CHOO ratio of 50:50 for *trans*-3-hexene, and 20:80 for *cis*-3-hexene. Campos-Pineda and Zhang (2017)
322 reported direct measurements of the vinyloxy radical formed in decomposition of *syn*-CH₃CHOO, from *cis*- and
323 *trans*-but-2-ene ozonolysis, inferring a yield of *syn*-CH₃CHOO of ~0.5 from *trans*-but-2-ene and ~0.3 from *cis*-
324 but-2-ene, broadly in line with estimations from measured OH yields.

325 Early theoretical calculations considering the gas phase (Cremer, 1981a,b) suggested that (*Z*)-RCHOO is
326 likely to be formed in greater yield for small alkenes, but that (*E*)-RCHOO becomes more favoured in the

Deleted: Piñeda

328 ozonolysis of large alkenes. Calculations by Rathman et al. (1999) suggested that (*Z*)-CH₃CHOO should be
329 favoured in *trans*-but-2-ene ozonolysis, but that conversely (*E*)-CH₃CHOO would be favoured in *cis*-but-2-ene
330 ozonolysis. Recent theoretical work (Watson, 2021) looking at POZ fragmentation for a series of disubstituted 2-
331 alkenes (CH₃CH=CHR), suggests formation of (*E*)-RCHOO will be strongly favoured in the ozonolysis of *cis*-
332 alkenes (87 % for *cis*-but-2-ene, increasing to 93 % for *cis*-2-hexene), while there is a roughly equal split from
333 ozonolysis of *trans*-alkenes. This is in qualitative agreement with the experimental work discussed above but
334 suggests a stronger preference than observed in the direct measurements of the vinyloxy radical by Campos-Pineda
335 and Zhang (2017). For tri-substituted alkenes, Watson (2021) finds a strong preference for formation of (*E*-
336 RCHOO on the mono-substituted side of the double bond. For the C₄-CI formed in isoprene ozonolysis, theoretical
337 calculations have determined a relative split of 50:50 for the two conformers of MVKO (Kuwata et al., 2005), and
338 20:80 for *syn*-MACRO:*anti*-MACRO (Kuwata and Valin, 2008). This is in qualitative agreement with the
339 observed low OH yield (0.08-0.13) from 1,3-butadiene (Atkinson and Aschmann, 1993; Kramp and Paulson,
340 2000) if it is assumed that decomposition of *syn*-MACRO will have a high OH yield whereas *anti*-MACRO will
341 not yield OH. To the authors' knowledge there is no other information on the relative yields of *syn/anti*-R₁R₂COO
342 (where R₁ ≠ R₂).

343 2.7 POZ ring opening to a biradical

344 In addition to direct CI + carbonyl formation from the POZ, the possibility exists of ring opening of the POZ to a
345 singlet alkoxy-peroxy biradical (>C(O[•])-C(OO[•]<)) (O'Neal and Blumstein, 1973; Olzmann et al., 1997; Anglada
346 et al., 1999; Fenske et al., 2000; Nguyen et al., 2015; Pfeifle et al., 2018) (Figure 4). In addition to re-closing the
347 ring to the POZ or decomposing to CI + carbonyl, this alkoxy-peroxy biradical can migrate an H-atom from the
348 alkoxy-bearing carbon, forming a carbonyl hydroperoxide (-C(=O)-C(OOH)<); this pathway is only possible if
349 the alkene has a vinylic H-atom. The carbonyl hydroperoxide formed has a high energy content, over 400 kJ mol⁻¹,
350 and can eliminate an OH radical, forming a α -carbonyl-alkoxy radical that rapidly decomposes to an acyl radical
351 and a carbonyl. This pathway has been invoked in theoretical studies as the main source of OH in the ozonolysis
352 of ethene (in which OH cannot be formed via a VHP) (Nguyen et al., 2015; Pfeifle et al., 2018), and is expected
353 to contribute somewhat to OH formation in other alkenes, though this has not yet been investigated experimentally
354 or theoretically. Alternative proposed sources of OH in ethene ozonolysis all involve the CH₂OO Criegee
355 intermediate. However, theory has shown that direct OH formation from CH₂OO by a 1,3-H-migration involves
356 too high a barrier (e.g. Nguyen et al., 2015; Pfeifle et al., 2018), while OH elimination from the hot formic acid
357 formed in the 1,3-ring closure (see Section 4.2) is not competitive against formation of H₂O + CO and H₂ + CO₂,
358 as also borne out by HCOOH pyrolysis experiments (Chang et al., 2007; Vichiatti et al., 2017). The carbonyl
359 hydroperoxide route thus resolves an apparent discrepancy between ethene ozonolysis experiments, which
360 observe significant OH yields, and experiments (Stone et al., 2018) and theoretical work (Nguyen et al., 2015;
361 Pfeifle et al. 2018), which indicate very little OH formation from CH₂OO. Pfeifle et al. (2018) calculated a yield
362 of 12.3 % for the carbonyl-hydroperoxide in ethene ozonolysis, while Nguyen et al. (2015) obtained 13 %, both
363 at the low end of the current IUPAC recommended OH yield (0.17±0.05) for the reaction (Cox et al., 2020).
364

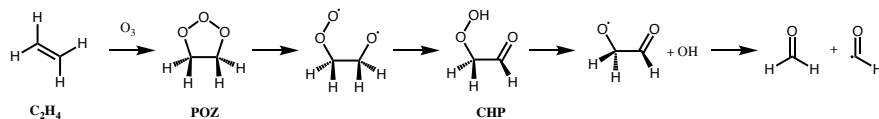
Deleted: Pineda

Deleted: Figure 4

Formatted: Font: 10 pt, Not Bold, Font colour: Black

Formatted: Font: 10 pt, Not Bold, Not Italic, Font colour: Black

Deleted: 100 kcal



369 **Figure 4. The carbonyl hydroperoxide (CHP) decomposition pathway for ethene ozonolysis**

371 **2.8 Protocol Rules for POZ fragmentation**

372 **2.8.1 POZ fragmentation**

373 A group contribution approach was designed to estimate POZ fragmentation yields. The approach assumes that
 374 the branching ratio for the two possible fragmentations of the POZ depends on the substituents of the
 375 $R_{1a}(R_{1b})C=C(R_{2a})R_{2b}$ parent alkene. The general form of the relationship is given by:

376

377
$$Y_{CI1} = \frac{(F_{1a}+F_{1b})-(F_{2a}+F_{2b})+1}{2} = 1 - Y_{CI2} \quad (E1)$$

378 where Y_{CI} is the CI production yield on the i^{th} carbon and F_R are the contributions for the 4 substituents on the
 379 C=C bond. The set of F_R values is developed based on the observed primary carbonyl yields (Supplementary
 380 Section S1 and Spreadsheet S1) and are based on a least squares fit to a relevant dataset of alkenes for each
 381 substituent (Figures S1-S5).

382 For a vinyl group, F is constrained to fit the IUPAC recommended yields of MVK and MACR from
 383 isoprene ozonolysis, assuming that ozone reacts 60% at the terminal double bond and 40% at the substituted
 384 double bond (Nguyen et al., 2016; Jenkin et al., 2020). The presence of a carbonyl group adjacent to the double
 385 bond appears to strongly favour formation of the opposing CI in the case of MVK (i.e. $-C(=O)CH_3$). However,
 386 this is not the case for other alkenes with the structure $-C(=O)R$ in the database, for which there appears to be no
 387 clear preference for formation of either CI, with a fit to the data yielding a slightly positive F value of 0.127. The
 388 strongest negative effect (i.e. most strongly favouring formation of the carbonyl containing the functional group)
 389 observed in the database is for enol ethers ($-OR$), giving an F value of -0.655. This is assumed to also be the same
 390 case for enols ($-OH$) based on the theoretical calculations of Lei et al. (2020) and Wang et al. (2020), and for vinyl
 391 esters ($-OC(=O)R$), based on the observed values for vinyl acetate. By contrast, an acrylate ester ($-C(=O)-OR$)
 392 substituent adjacent to the double bond does not appear to have a strong effect on fragmentation, and $F = 0$ is
 393 used. Similarly, the trend from the two unsaturated acids reported is unclear, and $F = 0$ is also used here. An OH
 394 group on the alpha carbon appears to slightly decrease Y_{CI} compared to an H atom, but the data is currently too
 395 limited to recommend a group additivity value, so the OH group is treated as an H atom, i.e. $F_{-CH_2OH} = F_{-CH_3}$.
 396 More distant oxygenated groups are not considered. The available data for exocyclic alkenes with the double bond
 397 attached to the ring is not able to take into account the effect of multiple rings, with F_{ring} being determined from
 398 only exocyclic alkenes with C_6 rings (β -pinene, methylene cyclohexane, and terpinolene). For rings with a vinyl
 399 group attached, $F_{(C_6)ring}$ is determined only from C_6 rings, i.e. styrene and vinylcyclohexane. Endocyclic alkenes
 400 are assumed to follow the same fragmentation patterns as acyclic alkenes. For example, cyclohexene is considered
 401 to have the structure $>CH_2CH_2CH=CHCH_2CH_2<$, 1-methyl cyclohexene $>CH_2CH_2C(CH_3)=CHCH_2CH_2<$ etc.

Deleted: H

Deleted: leading to

Deleted: -

405 The group contribution value, F , is then used in Eq. (1) to determine the yield of CI_1 (defined as having
 406 substituents 1a and 1b) from the general structure $R_{1a}(R_{1b})C=C(R_{2b})R_{2a}$. Generally, the measurement of the larger
 407 primary carbonyl was used to determine the primary carbonyl and CI yields. This is because in some cases, the
 408 smaller carbonyl can be formed as a decomposition product of the larger CI and hence is not a true primary
 409 carbonyl yield.

410

411

412

Table 1. Group contribution values (F) for various substituents

Group	Value	Alkenes used for fit
=ring	+ 0.62	β -pinene, methylene cyclohexane, terpinolene
-CH ₃	+ 0.218	propene, 2-methyl butene, 2-methyl-but-2-ene
-C(=O)R, -C(=O)H	+ 0.127	2-ethylacrolein, ethyl vinyl ketone, 4-hexen-3-one, 3-methyl-3-buten-2-one, 3-methyl-3-penten-2-one, 2-butenal, trans-2-hexenal
-CH ₂ CH ₃	+ 0.107	but-1-ene, 2-methyl-but-1-ene, 2-ethyl-but-1-ene, 2,2-dimethyl-hex-2-ene
-H	0	By definition
-COOH, -C(=O)-O-R,	0	Acids and acrylate esters, see spreadsheet S1
-CH ₂ CH ₂ R	0	pent-1-ene, hex-1-ene, hept-1-ene, oct-1-ene, dec-1-ene, 2-methyl-pent-1-ene
-CHR ₁ R ₂	- 0.069	3-methyl-but-1-ene, 3-methyl-pent-1-ene, 2,3-dimethyl-but-1-ene, 2,4-dimethyl-pent-2-ene, 2,3,4-trimethyl-pent-2-ene, 3-methyl-2-isopropyl-but-1-ene
-(C ₆)ring	- 0.25	styrene, vinyl cyclohexane
-vinyl	- 0.28	isoprene
-CR ₁ R ₂ R ₃	- 0.386	2,3,3-trimethyl-but-1-ene, 2,4,4-trimethyl-pent-2-ene, 2,2-dimethyl-hex-3-ene, 3,3-dimethyl-but-1-ene
-OR, -OH, -OC(=O)R	- 0.655	methyl vinyl ether, ethyl vinyl ether, propyl vinyl ether, butyl vinyl ether, ethyl propenyl ether

Deleted: (-

413 2.8.2 *E/Z* conformer yields

414 In light of the current paucity of experimental and/or theoretical information on the relative yields, an equal 0.5:0.5
 415 yield is assigned as a default value for (*E*)/(*Z*) isomers for all asymmetrical CI. The following two exceptions are
 416 nevertheless considered. For acyclic *cis*-RCH=CHR parent alkenes, a relative yield of 0.7:0.3 is set for (*E*):(*Z*) CI.
 417 For conjugated structures, formation of (*E*)/(*Z*)->C=C(R)-CHOO is assumed to be in a ratio of 0.8:0.2, based on
 418 the work of Kuwata et al. (2005) and Kuwata and Valin (2008).

419 2.8.3 Carbonyl-hydroperoxide route

420 While there is little information available on the stepwise carbonyl-hydroperoxide POZ decomposition
 421 mechanism, it is needed to account for the radical yields observed in the ozonolysis of ethene as discussed above.
 422 There is no reason to assume it will not occur more generally for any alkenes with vinylic H-atom(s), though
 423 perhaps with different fates of the intermediate biradical and/or carbonyl hydroperoxide (e.g. larger
 424 hydroperoxides could be more prone to collisional stabilisation and yield less prompt OH). Currently this channel
 425 is only included for the ethene-ozone reaction, for which it is assumed that 0.12 of the ethene-ozone reaction
 426 forms the biradical intermediate, rather than the CI + carbonyl, using the contribution calculated for the carbonyl
 427 hydroperoxide channel by Pfeifle et al. (2018). When more general data become available, assuming the channel
 428 is active for other systems, the protocol will be updated. The general structure of such a scheme might be: the
 429 POZ is assumed to break either of the O-O bonds with equal probability, forming one of two possible biradicals.
 430 If there is an available vinyl α -hydrogen, it is assumed that the H-shift to the peroxy radical occurs, forming the
 431 carbonyl-hydroperoxide ($R_1R_2C(OOH)C(=O)R_3$), followed by loss of OH and scission of the C-C bond to yield

433 the stable product $R_1R_2C=O$ and the radical $R_3C=O$. If there is no available α -hydrogen, the biradical is assumed
434 to yield the CI and carbonyl, either by C–C fragmentation or recyclisation to the POZ.

435 3 Stabilisation of the Criegee Intermediate

436 3.1 Excited vs. stabilised CI

437 Following decomposition of the primary ozonide, CI are formed with a broad range of internal energies (e.g.
438 Drozd et al., 2011). Consequently, it is often useful to consider the mean energy of a population of CI. Those
439 generated with a high internal energy, allowing prompt chemical reactions, are called excited, or chemically
440 activated CI (CI*). Those without enough internal energy to undergo prompt decomposition are considered to be
441 ‘stabilised’ CI (SCI). Additionally, CI* can be collisionally stabilised. This has been demonstrated by
442 experimental work showing that SCI yields are pressure dependent (Drozd et al., 2011, Hakala and Donahue,
443 2016; 2018). Note that this pressure dependence is moderate, and across the range of relevant atmospheric
444 pressures not of primary concern; we base our analysis on the available data near 1 atm.

445 3.2 SCI Yield

446 The total SCI yield for a given alkene is the sum of the fraction of the nascent CI population that is formed
447 stabilised, plus the fraction of CI* that is collisionally stabilised. The fate of the CI* is a competition between
448 prompt unimolecular decay and collisional stabilisation, with the CI* having a lifetime on the order of
449 nanoseconds against either of these processes (e.g. Drozd et al., 2017; Stephenson and Lester, 2020). Most alkenes
450 will form a number of different CI*, each with different lifetimes against unimolecular decay and collisional
451 stabilisation. The rate of collisional stabilisation of a given CI* is dependent on the frequency of collisions (and
452 hence pressure), and the efficiency of energy loss to the bath gas. The rate of unimolecular decay of a given CI*
453 depends on: (i) the energy of the CI* when formed, (ii) the activation energy for the most facile decay process /
454 the energy required for tunnelling, and (iii) the relative density of states of the reactants and transition state, i.e.
455 the entropy of the reaction. The dominant unimolecular decay mechanism is dependent on the structure of the CI;
456 these mechanisms are discussed in Section 5.

457 Larger CI* will tend to be stabilised to a greater extent due to a greater density of states distributing the
458 excess internal energy over a greater number of modes and so reducing the rate of unimolecular decay (Drozd and
459 Donahue, 2011; Stephenson and Lester, 2020). Hence, as the size of the CI increases relative to the carbonyl co-
460 product formed in POZ decomposition, the fraction of the energy taken by the CI from the POZ will increase
461 (assuming the energy has time to become equally distributed throughout the POZ), but typically the mean excess
462 energy per degree of freedom of the nascent CI population decreases, and hence the fraction of CI* with enough
463 energy to undergo unimolecular decay also decreases (Fenske et al., 2000; Newland et al., 2020). This will lead
464 to greater stabilisation, i.e. higher SCI yields. Similarly, for a given CI size, carbonyl co-products of increasing
465 size will take a larger fraction of the excess energy, leaving the CI* moiety with less energy and thus will also
466 lead to higher SCI yields (Newland et al., 2020). Conversely, for endocyclic alkenes, decomposition of the POZ
467 produces a single molecule containing both the carbonyl and carbonyl oxide moieties. Such CI have a high initial
468 energy, with no energy lost from the POZ decomposition to the carbonyl or to relative motion of the fragments,
469 and thus require many collisions to be quenched (Vereecken and Francisco, 2012). Consequently, endocyclic

Deleted: However

Deleted: CI

Deleted: decreasing

Deleted: F

474 alkenes with $\leq C_7$ have little stabilisation (Hatakeyama et al., 1984; Campos-Pineda and Zhang, 2017; Drozd and
 475 Donahue, 2011). For the endocyclic C_{10} monoterpenes α -pinene and limonene, total SCI yields have been
 476 measured to be 0.13-0.22 (Hatakeyama et al., 1984; Taipale et al., 2014; Sipilä et al., 2014; Newland et al., 2018)
 477 and 0.23-0.27 (Sipilä et al., 2014; Newland et al., 2018) respectively. For the C_{15} sesquiterpene β -caryophyllene,
 478 a total SCI yield (including from decomposition of the stabilised POZ) of 0.74 was calculated by Nguyen et al.
 479 (2009), with a value of > 0.6 determined experimentally (Winterhalter et al., 2009).

480 Total SCI yields have been measured experimentally for many alkene-ozone systems. These are generally
 481 determined indirectly, by performing ozonolysis experiments in the presence of an SCI scavenging species (e.g.
 482 H_2O , SO_2 , hexafluoroacetone). Measurements of scavenger removal, or formation of products from the SCI +
 483 scavenger reaction, are used to determine the SCI yield. Yields measured in such a way must be considered to be
 484 lower limits since, under most experimental conditions, a significant fraction of the SCI may undergo
 485 unimolecular decomposition based on recently reported fast SCI decomposition rates (e.g. Newland et al., 2015;
 486 Vereecken et al., 2017; Newland et al., 2018). The choice of scavenger species is also important. In some older
 487 experimental studies, water was used as an SCI scavenger, with H_2O_2 (e.g. Hasson et al., 2001a) or hydroxymethyl
 488 hydroperoxide (HMHP, e.g. Hasson et al, 2001a; Neeb et al., 1997) being the detected reaction products. For
 489 mono-substituted (*E*)-SCI, or for CH_2OO , this may be a reasonable assumption, with $k_{(H_2O+SCI)}/k_{(decomp.)} \sim$
 490 $10^2 - 10^3$ at $[H_2O] = 5 \times 10^{17} \text{ cm}^{-3}$ (e.g. Vereecken et al., 2017). However, for (*Z*)-SCI, $k_{(H_2O+SCI)}/k_{(decomp.)} \sim$
 491 $10^2 - 10^1$, i.e. the majority of the SCI will not be scavenged by H_2O .

492 3.3 Protocol Rules for CI Stabilisation

493 The relationship between stabilisation of the CI^* and size of the carbonyl co-product has been studied for CH_2OO
 494 and $(CH_3)_2COO$ by Newland et al. (2020) (Figure S). For CH_2OO this relationship might be expected to represent
 495 a minimum for CI^* that primarily decay via the 1,3 ring closure pathway (i.e. *anti*- CI^* , see Section 4.2), since
 496 larger CI^* will have a slower decay rate due to a greater density of states. Similarly, the trend for $(CH_3)_2COO$ can
 497 be assumed to be close to a minimum for CI^* that primarily undergo the 1,4 vinylhydroperoxide (VHP)
 498 decomposition pathway (see Section 4.1), with only *syn*- CH_3CHOO likely to have a lower density of states (and
 499 therefore faster decomposition) (Stephenson and Lester, 2020). With no further data available, the stabilisation
 500 trend of CH_2OO is used for CI^* that decompose via 1,3 ring closure, while that of $(CH_3)_2COO$ is used for CI^* that
 501 decay via the 1,4 vinylhydroperoxide pathway. For other pathways, such as the 1,5-ring closure to a dioxole (see
 502 Section 4.4), important in isoprene ozonolysis, no information is available. CI^* with a vinyl group *syn* to the
 503 terminal oxygen of the carbonyl oxide are considered as *syn*- CI for the purposes of calculating stabilisation in the
 504 protocol.

505 An extension of Equation E7 in Newland et al. (2020) is used to estimate the CI stabilisation S :

$$506 \quad S = 1 - \left[\left(\frac{A_{CI}}{A_{tot}} \right) \times F \times z_{path} \right] \quad (E2)$$

508 where A_{CI} is the total number of non-hydrogen atoms in the CI^* and A_{tot} is the total number of non-hydrogen atoms
 509 in the POZ. F_{13RC} and F_{VHP} are values determined for CH_2OO and $(CH_3)_2COO$, based on the SCI yields for their
 510 symmetrical parent alkenes ethene and 2,3-dimethylbut-2-ene, respectively. For CH_2OO this is 0.95 and for
 511 $(CH_3)_2COO$ it is 1.24 (Newland et al., 2020). In this work, an additional term, z_{path} , is included to take into account

Formatted: Font: 10 pt, Not Bold

Deleted: Figure 5

Formatted: Font: 10 pt, Not Bold, Not Italic

Deleted: ,

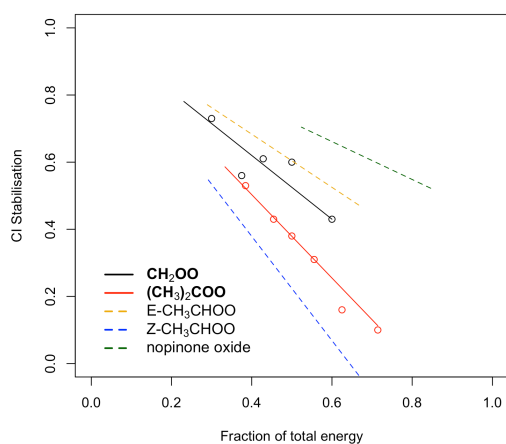
Deleted: ,

Deleted: and F_{VHP}

Deleted: F_{13RC}

517 the observed / predicted increased stabilisation of CI* with size. For CI* that decay via the 1,3 ring closure
 518 pathway, z_{13RC} is defined as $x / (A_{CI} + (x - A_{CH_2OO}))$, where A_{CH_2OO} is the total number of non-hydrogen atoms in
 519 CH_2OO (i.e. 3), and x is an adjustable parameter. For CI* that decay via the 1,4 H-shift, z_{VHP} is defined as $x / (A_{CI}$
 520 $+ (x - A_{(CH_3)_2COO}))$, where $A_{(CH_3)_2COO} = 5$. In both terms, $x = 5$, and has been optimized to improve the fit between
 521 measured and calculated total SCI yields of larger alkenes (Newland et al., 2020).

522 **Figure 5** shows the measured CI* stabilisation for CH_2OO and $(CH_3)_2COO$ as a function of the total
 523 energy taken from the POZ by the CI*, from Newland et al. (2020). Fits to the measured data are calculated using
 524 Eq. (2). Also shown are the calculated stabilisation trends for (*E*)- and (*Z*)- CH_3CHOO and nopinone oxide (the C_9
 525 CI* formed in β -pinene ozonolysis). **Figure 5** shows that stabilisation of *E*-CI* is predicted to be considerably
 526 greater than for *Z*-CI* when formed with the same energy. For CH_3CHOO it is noted that very little (0.11)
 527 stabilisation of (*Z*)- CH_3CHOO^* is predicted when produced from but-2-ene ozonolysis (fraction of total energy
 528 = $A_{CI}/A_{tot} = 4/7 = 0.57$), whereas a much greater stabilisation of (*E*)- CH_3CHOO^* is predicted. Using the *E/Z*-
 529 $RCHO$ yields given in Section 2.8.2 for *cis* and *trans* alkenes, and the trends presented in **Figure 5**, then a total
 530 SCI yield of 0.33 for *trans*-but-2-ene and 0.42 for *cis*-but-2-ene is calculated, in good qualitative agreement with
 531 the relationship observed in Newland et al. (2015). The calculated values for nopinone oxide demonstrate the
 532 decreasing sensitivity of CI* stabilisation to the co-product size as the size of the CI* increases.



533 **Figure 5.** Dependence of CI* stabilisation on the fraction of the total energy taken from the POZ. Black (CH_2OO) and
 534 red ($(CH_3)_2COO$) points, measurements taken from Newland et al. (2020). Solid and dashed lines, fits calculated using
 535 Eq. (2).
 536

537 For endocyclic alkenes, an empirically derived sigmoid fit (Supplementary Section S2: Equation S1; Figure
 538 S6) is applied to the very limited dataset that shows $Y_{SCI} \approx 0$ for $C \leq 7$, $Y_{SCI} \approx 0.2$ for monoterpenes, and $Y_{SCI} \approx$
 539 0.74 for sesquiterpenes.

540 4 Unimolecular reactions of CI* and SCI

541 CI can undergo unimolecular isomerisation / decomposition. The unimolecular pathways available to SCI are
 542 assumed to be the same as those available to CI* (although it is noted that there is little evidence to back up this

Formatted: Font: 10 pt, Not Bold

Deleted: Figure 5

Formatted: Font: 10 pt, Not Bold, Not Italic

Formatted: Font: 10 pt, Not Bold

Formatted: Font: 10 pt, Not Bold, Not Italic

Deleted: Figure 5

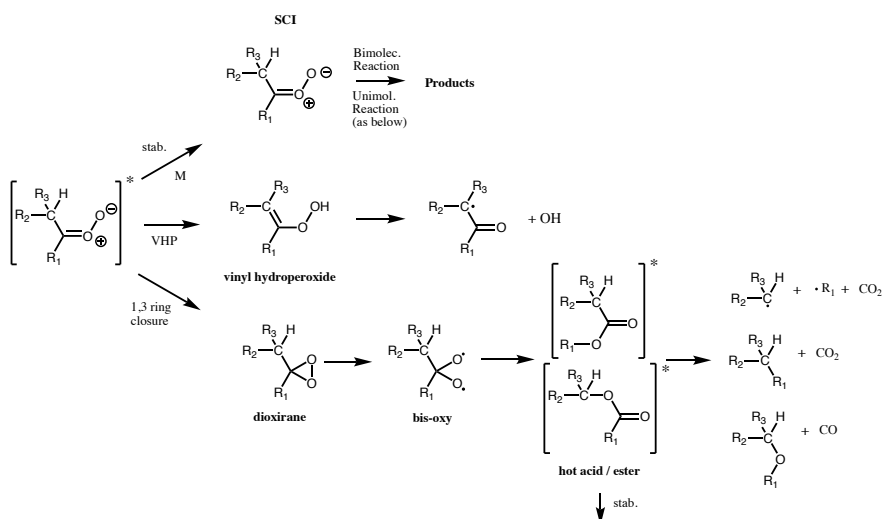
Formatted: Font: 10 pt, Not Bold, Not Italic

Deleted: Figure 5

Formatted: Font: 10 pt, Not Bold

546 assumption). However, while for CI* these processes are prompt, occurring on a timescale of 10^{-9} s (Drozd et al.,
 547 2017), for SCI they occur at a range of rates such that their competition with atmospheric bimolecular reactions
 548 needs to be considered. A wide range of unimolecular isomerisation / decomposition pathways have been
 549 characterised for CI, but only two of these are believed to be important for saturated CI under atmospheric
 550 boundary layer conditions (Vereecken et al., 2017): a 1,4 H-migration, i.e. the vinylhydroperoxide pathway, and
 551 a 1,3 ring closure, i.e. the hot acid / ester pathway (Figure 6). If the vinylhydroperoxide pathway is available, then
 552 this will always be the dominant decomposition pathway as it is the energetically most facile, with only a slight
 553 entropic disadvantage compared to the 1,3 ring closure (Vereecken et al., 2017). Unsaturated CI have some
 554 additional pathways available (see Section 4.4).

555 Experimentally determined decomposition rates are available only for a limited number of SCI. Early
 556 estimates were considerably slower than more recent experimental evidence. Vereecken et al. (2017) recently
 557 published an extensive SAR providing temperature dependent unimolecular rates and mechanisms for a wide
 558 range of SCI structures based on theoretical calculations tied to experimental work as well as group additivity
 559 relations.



560

561 **Figure 6.** Available pathways for a CI with a hydrogen atom available in beta position to the carbonyl oxide. From top
 562 to bottom, the available pathways are the stabilisation (stab.) pathway, the vinylhydroperoxide (VHP) pathway and
 563 the 1,3 ring closure (hot acid/ester) pathway.

564 4.1 Vinylhydroperoxide (VHP) pathway

565 A CI with a β -hydrogen atom in a *syn* orientation to the terminal oxygen atom of the carbonyl oxide can isomerise
 566 to form a vinylhydroperoxide via a 5-membered transition cycle (Figure 6). This route is therefore available to
 567 monosubstituted (*Z*)-CIs and disubstituted CIs. The VHP formed has a short lifetime and promptly or thermally
 568 decomposes to form an OH radical and a β -acylalkyl (vinoxy) radical, in some cases with a small yield of β -acyl-
 569 alcohols (Taatjes et al., 2016; Kuwata et al., 2018). The OH radicals are thus formed on a short time scale (e.g.
 570 Drozd et al., 2017) directly from the VHP decomposition. The β -acylalkyl radical reacts with O_2 to form a β -

Formatted: Font: 10 pt, Not Bold

Formatted: Font: 10 pt, Not Bold, Not Italic

Deleted: Figure 6

Formatted: Font: 10 pt, Not Bold

Formatted: Font: 10 pt, Not Bold, Not Italic

Deleted: Figure 6

573 acylperoxy radical. On a longer timescale, the subsequent chemistry of this peroxy radical can yield further HO₂
574 and OH radicals (e.g. Nguyen et al., 2016).

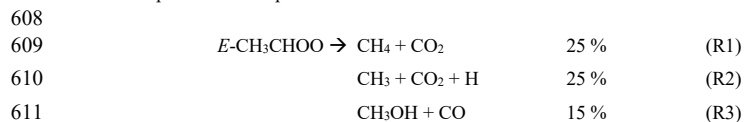
575 The best studied system that follows the 1,4 H-shift pathway is stabilised (CH₃)₂COO. Experimentally
576 derived rates are fast (300 – 1000 s⁻¹) (Berndt et al., 2014b; Newland et al., 2015; Chhantyal-Pun et al., 2016;
577 Smith et al., 2016). The experimental evidence also shows a strong temperature dependence, with measured rates
578 varying from 269 s⁻¹ at 283 K to 916 s⁻¹ at 323 K (Smith et al., 2016). This is in good agreement with the SAR of
579 Vereecken et al. (2017) which shows that the rate of decomposition of saturated SCI is fastest (*ca.* 500 s⁻¹) for
580 those SCI with access to the VHP route. This SAR shows that the rate is slowed by more than an order of
581 magnitude when only one H atom is available on the α -carbon and that the rates are also affected by the *anti*-
582 substituent, with the presence of a vinyl group reducing rates by an order of magnitude, and the presence of a
583 carbonyl group reducing rates by two orders of magnitude.

584 This pathway may not be available to certain CI structures even though there is an available hydrogen on
585 the α -carbon. This is the case for the bicyclic C₉ CI formed in ozonolysis of the monoterpene β -pinene, with the
586 terminal oxygen facing the four membered ring. Calculations have shown that formation of the vinyl
587 hydroperoxide is not possible for this CI due to the strain it would put on the ring, and so the dominant
588 decomposition pathway is 1,3 ring closure (Nguyen et al., 2009b). This has also been shown to be the case for the
589 cyclic C₉ CI formed facing the three membered ring in the ozonolysis of sabinene (Almatarneh et al., 2019).

590 4.2 1,3 ring closure

591 For monosubstituted (*E*)-CI and CH₂OO (see Section 5.3), decomposition via a VHP is not available. Instead
592 unimolecular reaction proceeds predominantly via a 1,3 ring closure, with typical rates $\leq 10^2$ s⁻¹ (Vereecken et al.
593 2017), to a chemically activated dioxirane species (Figure 6). This breaks the weak O-O bond giving a singlet bis-
594 oxy radical (Wadt and Goddard, 1975; Herron and Huie, 1977; 1978). Various pathways have been proposed for
595 the subsequent chemistry of this species based on observed product distributions (Chen et al., 2002). This pathway
596 has been characterised best for CH₂OO (Section 5.3). The dioxirane is thought to rearrange to a 'hot' acid / ester,
597 which can undergo decomposition to yield a range of products. As the size of the CI increases, the hot acid / ester
598 is predicted to be more likely to be collisionally stabilised (Vereecken and Francisco, 2012).

599 There have been very few experimental studies to date on the products of isomerisation / decomposition
600 of (*E*)-RCHOO. This is challenging experimentally as (*E*)-RCHOO will always be formed as a partner with (*Z*)-
601 RCHOO. The most studied (*E*)-CI is (*E*)-CH₃CHOO, with observed products from *cis/trans*-but-2-ene ozonolysis
602 (which yields (*E*)- and (*Z*)-CH₃CHOO as the CI products) of HCHO, CH₃COOH, CH₃OH, CH₄, CHOCHO,
603 ketene, CO and CO₂ (e.g. Tuazon et al., 1997; Grosjean et al., 1994). With the exception of glyoxal, these can all
604 be rationalised as decomposition products of 'hot' (*E*)-CH₃CHOO via various pathways (Reactions R1 – R5). The
605 relative proportion of each channel is based on the reported yields in Tuazon et al. (1997), except for CH₃COOH,
606 from Grosjean et al. (1994), although it is noted that CH₃COOH may be a product of CH₃CHOO + water vapour
607 in their experimental setup.



Deleted:

Formatted: Font: 10 pt, Not Bold

Deleted: Figure 6

Formatted: Font: 10 pt, Not Bold, Not Italic

614	$\text{H}_2\text{CCO} + \text{H}_2\text{O}$	10 %	(R4)
615	CH_3COOH	20 %	(R5)

616

617 For $\text{R}_1\text{R}_2\text{COO}$ decomposition via 1,3 ring closure, products are formed via a 'hot' ester. There has been very little
618 work on the relative contribution of decomposition channels and stabilisation for these species. For example, there
619 is no experimental work to validate the predicted trend of increasing stabilisation of the hot acid / ester with size,
620 or at what size this becomes important. For the large terpenoid compounds β -pinene (Nguyen et al., 2009b) and
621 β -caryophyllene (Nguyen et al., 2009a), the acids/lactones formed from isomerisation of the C_9 -dioxirane have
622 been predicted to be fully stabilised.

623

624

625 4.3 CH_2OO

626 CH_2OO also follows the 1,3-ring closure pathway but is considered separately here as it has been the subject of a
627 considerable body of work. Experimentally reported products from CH_2OO decomposition include: CO_2 , CO , H_2 ,
628 OH , HO_2 , H_2O , and HCOOH (e.g. Calvert et al., 2000). Recent theoretical (Nguyen et al., 2015; Stone et al., 2018;
629 Peltola et al., 2020) works suggest that the only reaction pathway of the bis-oxy radical important under
630 tropospheric conditions is isomerisation to 'hot' formic acid, followed by decomposition to either $\text{H}_2 + \text{CO}_2$ or
631 $\text{H}_2\text{O} + \text{CO}$, in agreement with experimental and theoretical work on acid pyrolysis experiments (Chang et al.,
632 2007; Vichiatti et al., 2017). Due to the large excess energy and its small size, very little of the hot acid is stabilised,
633 with measured HCOOH yields from ethene ozonolysis < 5% (Calvert et al., 2000) (and the latter may be due to
634 bimolecular reactions of SCI rather than stabilisation of the hot acid). Stone et al. (2018) and Peltola et al. (2020)
635 considered the decomposition of stabilised CH_2OO using master equation simulations, determining the major
636 decomposition channel to be $\text{H}_2 + \text{CO}_2$ (64 % and 61% respectively), with the $\text{H}_2\text{O} + \text{CO}$ accounting for the
637 remainder (36%) in Stone et al. (2018), while Peltola et al. (2020) also found a small contribution (~8%) from the
638 $\text{OH} + \text{HCO}$ channel. It is noted that previous experimental work on ethene ozonolysis (Su et al., 1980; Horie et al.,
639 1991; Neeb et al., 1998) has generally inferred a preference for the $\text{H}_2\text{O} + \text{CO}$ channel. This may be due to different
640 pathways being followed by the dioxiranes formed from the excited CH_2OO produced in the ozonolysis reaction
641 compared to those formed from stabilised CH_2OO , as suggested by work on larger systems (Nguyen et al., 2009a;
642 2009b), and in the calculations of Nguyen et al. (2015) on excited CH_2OO decomposition in ethene ozonolysis. A
643 decomposition pathway to $\text{HCO} + \text{OH}$, proposed as the source of observed OH yields of 8-15 % in earlier
644 experimental studies on the ozonolysis of ethene (Gutbrod et al., 1997; Rickard et al., 1999; Kroll et al., 2001;
645 Alam et al., 2011) and larger alkenes (Kroll et al., 2002), has recently been determined experimentally to be
646 negligible (Stone et al., 2018), accounting for less than 2 % of the overall decay. This is in agreement with earlier
647 theoretical work (Olzmann et al., 1997; Nguyen et al., 2015) suggesting negligible OH yields from ethene
648 ozonolysis. This apparent discrepancy between experiment and theory can be reconciled by invoking the
649 possibility of OH formation via the carbonyl-hydroperoxide channel in the POZ decomposition, as discussed in
650 Section 2.7.

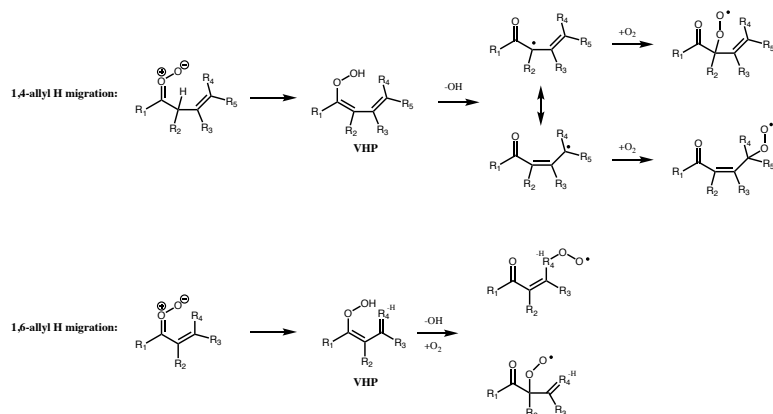
651 The unimolecular decomposition rate of stabilised CH_2OO has been experimentally determined to be very
652 slow ($< 12 \text{ s}^{-1}$) (Berndt et al., 2015; Chhantyal-Pun et al., 2015; Newland et al., 2015; Stone et al., 2018; Peltola et

653 al., 2020), with a current recommendation by IUPAC of $\leq 0.2 \text{ s}^{-1}$ at 1 bar and 298 K (Cox et al., 2020). Even at
 654 the upper end of these estimates, decomposition is a negligible atmospheric fate for stabilised CH_2OO compared
 655 to reaction with water vapour.

656 4.4 Unimolecular reactions of unsaturated CI

657 The ozonolysis of conjugated alkenes proceeds via the same initial POZ mechanism as non-conjugated systems,
 658 but decomposition of the POZ leads to the formation of unsaturated CI and/or carbonyls. While many of the
 659 characteristics of the chemistry are expected to be similar, the theoretical work of Kuwata et al., (2005), Kuwata
 660 and Valin (2008), and Vereecken et al. (2017) has shown some important differences. Specifically, additional
 661 unimolecular decomposition channels (Figure 7 and Figure 8) become available, which in some cases are faster
 662 than the 1,4 H-shift channel.

663



664

665 **Figure 7. Dominant unimolecular decomposition routes available to unsaturated CI with the terminal oxygen *syn* to an**
 666 **α or β vinyl group. Pathways available if terminal oxygen is *anti* to a vinyl group are the same as for saturated CI. For**
 667 **1,5-ring closure see Figure 8.**

668 If the vinyl group of an unsaturated CI is *anti* to the terminal oxygen of the carbonyl oxide, then the molecule will
 669 follow one of the two routes available to saturated CI, but with a rate affected by the presence of the double bond.
 670 However, if the vinyl group is *syn* to the terminal oxygen, alternative mechanisms of decomposition are available.
 671 1,4 and 1,6-allyl H-migration (for the vinyl group being in β or α position respectively), are available if an H atom
 672 is present on the α or γ carbon. These pathways lead to similar products to 1,4-alkyl H-migration, with a
 673 vinylhydroperoxide intermediate decomposing to give OH and one of two possible unsaturated peroxy radicals.
 674 If no H-atom is available for (*Z*)- β -unsaturated CI then they follow the 1,3-ring closure channel with SCI
 675 decomposition rates $\leq 1 \text{ s}^{-1}$. The rates of the 1,6-allyl H-migration channel for SCI are of the order of 10^6 s^{-1} , while
 676 1,4-allyl H-migration of SCI has rates ranging from $10^1 - 10^4 \text{ s}^{-1}$ depending on other substituents (Vereecken et
 677 al. 2017).

Formatted: Font: 10 pt, Not Bold

Formatted: Font: 10 pt, Not Bold, Not Italic

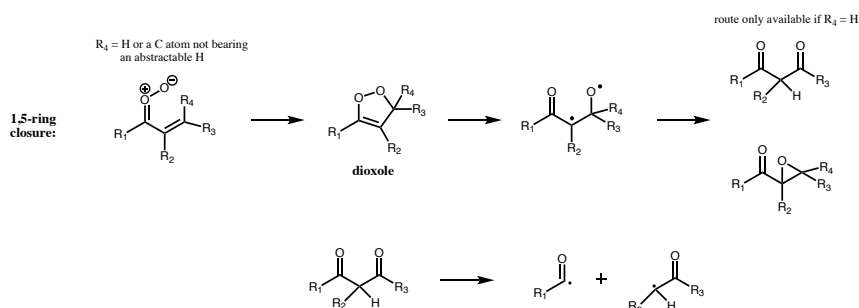
Deleted: Figure 7

Formatted: Font: 10 pt, Not Bold, Font colour: Black

Formatted: Font: 10 pt, Not Bold, Not Italic, Font colour: Black

Deleted: Figure 8

680 For CI with the carbonyl oxide *syn* to an α vinyl group, and without an available hydrogen on the α
 681 carbon, then the dominant decomposition mechanism is 1,5 ring closure, originally proposed by Kuwata et al.
 682 (2005) (Figure 8). This forms an intermediate dioxole species with a five membered ring. This is predicted to have
 683 high internal energy and to break the O-O bond, leading to an epoxy carbonyl, or, if $R_4 = H$, to a dicarbonyl
 684 (Kuwata 2005). The dicarbonyl has been predicted to undergo further prompt decomposition via various possible
 685 unimolecular channels, some of which appear to yield OH (Barber et al., 2018). Based on the stable product
 686 distribution from *anti*-MVKO decay, the decomposition of the dicarbonyl has been determined to be
 687 predominantly via C-C cleavage leading to two radicals (acetyl and vinoxy radicals in the case of *anti*-MVKO)
 688 (Vansco et al., 2020). These radicals will add O_2 leading to RO_2 radicals which may undergo further
 689 decomposition if formed chemically excited, ultimately to $HCHO + OH + CO$ in both cases (Carr et al., 2011;
 690 Weidman et al., 2018; Vansco et al., 2020). For *syn*-MACRO, Vansco et al. (2020) determine a pathway via a
 691 dioxole analogous to that just described, leading to formyl and 2-methyl vinoxy radicals, the latter of which could
 692 ultimately yield $CH_3CHO + OH + CO$. However, this accounts for only about half of the decomposition of the
 693 dicarbonyl, with the other half leading to acrolein via an unidentified unimolecular process. It is noted that Barber
 694 et al. (2018) and Vansco et al. (2020) did not consider the epoxide isomerisation pathway for the dioxole. The
 695 calculated unimolecular decay rates for the dioxole forming pathways from *syn*-MACRO and *anti*-MVKO are
 696 fast, Vereecken et al. (2017, Table 25 in the supplementary material) reported a rate of 2500 and 7700 s^{-1} ,
 697 respectively, with increasing substitution on the vinyl group accelerating the reaction further, while Barber et al.
 698 (2018) reported a somewhat slower rate for *anti*-MVKO of 2140 s^{-1} . Decay of stabilized *syn*-MVKO is relatively
 699 slow at $33 - 50 \text{ s}^{-1}$ (Vereecken et al., 2017; Barber et al., 2018) making it a potentially important bimolecular
 700 reaction partner in the atmosphere.
 701



702

703 **Figure 8. 1,5-ring closure: dominant unimolecular pathway for unsaturated CI with the terminal oxygen *syn* to an α**
 704 **vinyl group and R_4 is not a carbon with an abstractable hydrogen.**

705 4.5 Protocol Rules for CI decomposition

706 For unimolecular decomposition of CI, the SAR of Vereecken et al. (2017) is used to determine decomposition
 707 pathways and rates (for SCI). The products from each decomposition pathway are given in Table 2, where any
 708 secondary reactions such as recombination with O_2 are already accounted for. The vinylhydroperoxide pathway
 709 is assumed to lead exclusively to a β -oxo alkyl radical and OH. For decomposition via 1,3 ring closure, the hot
 710 acid / ester formed is considered to decompose via one of the three major pathways determined for (*E*)-RCHOO:

Formatted: Font: 10 pt, Not Bold, Font colour: Black

Deleted: Figure 8

Formatted: Font: 10 pt, Not Bold, Not Italic, Font colour: Black

Deleted: 13,400

Formatted: Font: 10 pt, Not Bold

Formatted: Font: 10 pt, Not Bold, Not Italic

Deleted: Table 2

714 RH + CO₂ (40%), ROH + CO (20%), R + HO₂ + CO₂ (40%), based on the observed product yields from *cis* and
 715 *trans* but-2-ene experiments by Tuazon et al. (1997). While it is noted that Grosjean et al. (1994) observed a
 716 CH₃COOH yield of ~20%, this could also be a product of CH₃CHOO + water vapour in their experimental setup.
 717 For larger CI ($\geq C_9$) the acid / ester is considered to be fully stabilised, if two esters can be formed they are
 718 considered equally likely. This is recognised as an area where detailed experimental studies are required, to
 719 establish the sensitivity of acid / ester stabilisation to CI size, as well as identifying decomposition products for a
 720 range of CI sizes / structures, and whether these are different for chemically activated / thermalized dioxiranes, as
 721 predicted (Anglada et al., 1998; Nguyen et al., 2009a, 2009b). For CH₂OO decomposition, the protocol assigns
 722 the products equally to two decomposition pathways: H₂+CO₂ and H₂O+CO; as discussed above, no OH is formed
 723 directly.

724 For 1,4-and 1,6 allyl H-migration in unsaturated CI (Figure 7), formation of the alkyl radicals from each
 725 of the delocalized radical sites formed after OH elimination is assumed to be equally likely. The product yields
 726 given in Table 2 are for mechanisms that do not explicitly preserve stereo-specificity. For systems that track
 727 stereo-specific substitution on double bonds, H-migration is only possible from the *Z*-substituent, and the number
 728 of products is reduced accordingly, with a concomitant adjustment of the product yields.

729 For 1,5 ring closure (Figure 8), formation of the epoxide or the dicarbonyl are considered equally likely.
 730 The dicarbonyl undergoes further decomposition to yield two RO₂ following Barber et al. (2018). Unimolecular
 731 reaction rates for stabilised unsaturated CI are taken from the Vereecken et al. (2017) SAR. Clearly there remains
 732 much uncertainty on the proposed kinetics, and systematic experimental work on SCI yields, and final product
 733 studies of ozonolysis of conjugated alkenes is required to improve the proposed protocol.

734 Table 2. Decomposition pathways and products for CI in the protocol

Decomposition Pathway	CI Structure	Products
1,4 H-shift (VHP)		
1,3 ring closure (hot acid / ester) CI < C₉		R ₁ R ₂ + CO ₂ (40 %) R ₁ OR ₂ + CO (20 %) R ₁ + R ₂ + CO ₂ (40 %)
1,3 ring closure (hot acid / ester) CI ≥ C₉		R ₁ CO-O-R ₂ (50%) R ₁ -O-COR ₂ (50%)
CH₂OO		H ₂ +CO ₂ (50 %) H ₂ O+CO (50 %)
1,5-ring closure	R ₄ = H or a C atom not bearing an abstractable H 	
1,5-ring closure (R₃ = H)	R ₄ = H or a C atom not bearing an abstractable H 	(50%) R ₁ C(O)O ₂ + CHOC(O ₂)R ₂ (50%)

Formatted: Font: 10 pt, Not Bold

Deleted: Figure 7

Formatted: Font: 10 pt, Not Bold, Not Italic

Formatted: Font: 10 pt, Not Bold

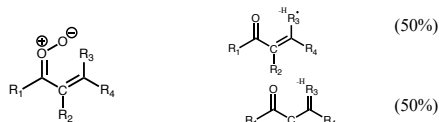
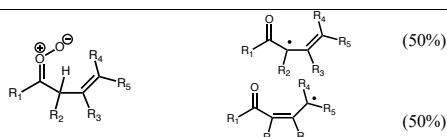
Formatted: Font: 10 pt, Not Bold, Not Italic

Deleted: Table 2

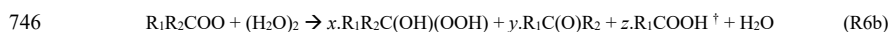
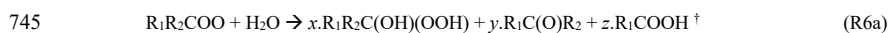
Formatted: Font: 10 pt, Not Bold, Not Italic, Font colour: Black

Deleted: Figure 8

Formatted: Font: 10 pt, Not Bold, Font colour: Black

1,6 allyl H-shift**1,4 allyl H-shift****738 5 Bimolecular Reactions of SCI**

739 Based on the unimolecular pathways described in Section 5, many SCI have lifetimes against unimolecular
 740 reaction on the order of $10^{-3} - 10^{-1}$ s. These lifetimes are long enough to allow them to participate in bimolecular
 741 reactions with trace gases in the atmosphere under typical boundary layer conditions, where Vereecken et al.
 742 (2017) estimated that just under half of the CI in the atmosphere react with a co-reactant rather than
 743 unimolecularly. The co-reactants for which fast reactions, of potential tropospheric importance, have been
 744 demonstrated are H_2O , $(H_2O)_2$, SO_2 , NO_2 , and organic and inorganic acids (Reactions 6 – 11).



747 † only available if $R_2 = H$



753 Reactions with other trace gases have been investigated both experimentally and theoretically, but these are not
 754 included in the protocol at this time as they are not considered to be important under tropospheric conditions.
 755 Theoretical and experimental work has also shown that more complex bimolecular and unimolecular pathways
 756 may operate forming heterocyclic molecules like cyclic peroxides and secondary ozonides (Chuong et al., 2004;
 757 Long et al., 2019). Again though, these reactions appear to be of negligible importance in the gas phase for SCI
 758 with carbon numbers up to C_{10} (monoterpenes) and are not considered in this protocol. While only reactions
 759 relevant to the atmosphere are included in the protocol; reactions that are not expected to be relevant in the
 760 atmosphere are still maintained in the database since they may be useful to interpret results of chamber simulations
 761 or other laboratory experiments (e.g. self-reaction or reaction with parent alkenes).

762 CH_2OO and (*E*)-RCHOO react rapidly with H_2O (Reaction R6a) (Welz et al., 2012; Taatjes et al., 2013;
 763 Stone et al., 2014) and with the water dimer, $(H_2O)_2$, (Reaction R6b) (Berndt et al., 2014a; Chao et al., 2015;
 764 Lewis et al., 2015; Lin et al., 2016), such that removal by water vapour is their predominant fate in the atmosphere.
 765 However, (*Z*)-RCHOO react slowly with H_2O (Taatjes et al., 2013; Sheps et al., 2014; Huang et al., 2015)
 766 increasing the importance of bimolecular reactions with other atmospheric trace species such as acids and SO_2

Deleted: O

Formatted: Subscript

Deleted: O

Deleted: O

770 (Newland et al., 2018). The reaction of SCI with organic acids (Reaction R7) is also likely to be an important
771 reaction in the atmosphere (Welz et al., 2014). The experimentally determined reaction rates for SCI + HCOOH
772 and CH₃COOH are $1 - 5 \times 10^{-10} \text{ cm}^3 \text{ s}^{-1}$ (Welz et al., 2014; Sipilä et al., 2014; Chung et al., 2019), close to the
773 collisional limit. Other potentially important reactions in the atmosphere include those with SO₂ (Reaction R8),
774 NO₂ (Reaction R9), and inorganic acids (Reactions R10-R11). The rates of SCI+SO₂ reaction have been the
775 subject of several studies for the three smallest SCI, with good agreement between experiments. Larger SCI appear
776 to have similar reaction rates with SO₂ (Ahrens et al., 2014).

777 The products of many of the bimolecular reactions of SCI are still uncertain. This is the case for the most
778 important bimolecular reactions in the atmosphere, those with H₂O and (H₂O)₂. A recent experimental study
779 (Sheps et al., 2017) of the reaction of CH₂OO with the (H₂O)₂, generating CH₂OO from the photolysis of
780 diiodomethane, determined yields of: hydroxymethylhydroperoxide (HMHP) (55 %), HCHO (40 %), and
781 HCOOH (5 %). However, ozonolysis experiments (e.g. Nguyen et al., 2016) have generally found HMHP and
782 HCOOH to be the main detected products, with negligible yields of HCHO. Based on results from isoprene
783 ozonolysis chamber experiments, Nguyen et al. (2016) proposed yields from the CH₂OO + H₂O reaction of:
784 HMHP (73 %), HCOOH (21 %), HCHO (6 %); and from the (H₂O)₂ reaction of: HMHP (40 %), HCOOH (54 %),
785 HCHO (6 %). These low HCHO yields are in agreement with earlier work (Hasson et al., 2001b) that determined
786 an HCHO yield of 6 – 9 %.

787 The products of SCI reaction with organic acids appear to be mainly hydroperoxide esters (Reaction R7).
788 Hydroperoxy methyl formate (HPMF) has been detected as an intermediate in the CH₂OO+HCOOH reaction (e.g.
789 Neeb et al., 1995; Wolff et al., 1997; Hasson et al., 2001a; Chung et al., 2019), hydroperoxy methyl acetate in the
790 CH₂OO+CH₃COOH reaction (Neeb et al., 1996), and hydroperoxy ethyl formate in the CH₃CHOO+HCOOH
791 reaction (Neeb et al., 1995; 1996; Cabezas and Endo, 2020). Theoretical calculations have predicted the formation
792 of > 90 % HPMF for the reaction of CH₂OO with HCOOH (Vereecken, 2017), and that the production of stabilised
793 hydroperoxide esters will be even higher for larger SCI. The reaction with SO₂ has been shown to form SO₃ with
794 close to unit yield (Reaction R8) (Kuwata et al., 2015). For NO₂, while early experimental work (Ouyang et al.,
795 2013) suggested SCI would oxidise NO₂ to NO₃, more recent experimental (Caravan et al., 2017) and theoretical
796 (Vereecken and Nguyen, 2017) work has suggested the formation of a nitroalkylperoxy radical (R₁R₂C(O₂)NO₂).
797 Subsequent reaction and formation of the alkoxy radical would be expected to yield a carbonyl and NO₂. The
798 main products of reaction of SCI with the inorganic acid HCl have been predicted to be chlorohydroperoxides
799 (Reaction R10) (Foreman et al., 2016; Vereecken, 2017), with these products observed experimentally for
800 CH₂OO+HCl (Cabezas and Endo, 2017; Taatjes et al., 2021) and CH₃CHOO+HCl (Cabezas and Endo, 2018).
801 The main product of reaction with HNO₃ has been predicted to be hydroperoxynitrates (Reaction R11) (Foreman
802 et al., 2016; Raghunath et al., 2017; Vereecken, 2017). Raghunath et al. (2017) further predicted decomposition
803 of a fraction of the chemically activated hydroperoxynitrates to CH₂(O)NO₃ + OH. This reaction has not yet been
804 studied experimentally to the authors' knowledge.

805 5.1 Protocol Rules for SCI Bimolecular Reactions

806 Bimolecular reaction rate coefficients for SCI are included for reaction with water vapour monomers and dimers,
807 SO₂, NO₂, carboxylic acids and inorganic acids (HCl, HNO₃) (Table 3). For the water vapour reactions, the rate
808 coefficients are taken from the SAR of Vereecken et al. (2017), which provides values for 98 explicit structures.

Formatted: Font: 10 pt, Not Bold

Formatted: Font: 10 pt, Not Bold, Not Italic

Deleted: Table 3

810 For bimolecular reactions of SCI with the other trace gases, four classes of SCI are considered: CH₂OO, *Z/E*-
 811 RCHOO and R₁R₂COO (where R represents alkyl groups), based on the limited experimental data available. The
 812 rates are taken from IUPAC recommendations (Cox et al., 2020) where available, otherwise from sources as stated
 813 in Table 3. Where the structure does not fit into the defined classes, the CH₂OO rate constant is attributed by
 814 default. Reaction products are as given in Reactions R6 – R11. In light of the current uncertainties of the product
 815 distribution of the reactions of SCI with water, here we assume the same products for the monomer and dimer
 816 reactions. We propose yields based on the direct study of Sheps et al. (2017) of α -hydroxyhydroperoxide (55 %),
 817 carbonyl (40 %) and acid (5 %), with the exception of R₁R₂COO, which cannot form the acid, for which we
 818 increase the α -hydroxyhydroperoxide to 60 %. These recommendations will be subject to change upon further
 819 experimental information becoming available.

820

821 **Table 3. Bimolecular reaction rates with RCOOH, SO₂, NO₂ and inorganic acids applied to the four SCI structures.**
 822 Rates are IUPAC recommendations (Cox et al., 2020) unless otherwise stated. Bimolecular reaction rates with water
 823 are taken from Vereecken et al. (2017), see main text.

	Bimolecular reaction rates (10 ¹¹ cm ³ molecules ⁻¹ s ⁻¹)				
	RC(O)OH	SO ₂	NO ₂	HCl ^a	HNO ₃ ^a
CH ₂ OO	12	3.7	0.3	4.6	54
(<i>E</i>)-RCHOO ^b	38 ^c	14	0.2	4.6	54
(<i>Z</i>)-RCHOO ^b	21 ^c	2.6	0.2	4.6	54
R ₁ R ₂ COO	31	16	0.2	4.6	54

824 ^a All values for CH₂OO reaction from Foreman et al. (2016); ^b IUPAC recommended values for (*E*) and (*Z*)-CH₃CHOO; ^c
 825 Mean of IUPAC recommended values for reaction with HCOOH and CH₃COOH.
 826

827 6 Example of protocol application

828 An example is described below for the unsaturated ketone, 6-methyl-5-hepten-2-one, and illustrated in Figures 9
 829 and 10. Further examples for α -pinene, *cis*-2-pentene, 2-methyl-1-pentene and 2-methyl-1,3-butadiene (isoprene)
 830 are given in the Supplementary (Section S3). The initial rate of reaction with ozone is defined by the protocol in
 831 the companion paper (Jenkin et al., 2020). The branching ratio for formation of the disubstituted CI* is calculated
 832 to be 0.72 using the group additivity values in Table 2 and Eq. (1).
 833

$$834 Y_{CI1} = \frac{(0.218+0.218)-(0+0)+1}{2} = 0.72 = 1 - Y_{CI2} \quad (E3)$$

835

836 The *syn* and *anti*-conformers of the two large CI* are formed with equal yield (0.14).

837 Stabilisation of each CI* is computed using Eq. (2):

838

$$839 (CH_3)_2COO: \quad S = 1 - \left[\left(\frac{5}{12} \right) \times 1.242 \times \left(\frac{5}{5+(5-5)} \right) \right] = 0.48 \quad (E4)$$

$$840 (Z)-CH_3C(O)(CH_2)_2CHOO: \quad S = 1 - \left[\left(\frac{8}{12} \right) \times 1.242 \times \left(\frac{5}{8+(5-5)} \right) \right] = 0.48 \quad (E5)$$

$$841 (E)-CH_3C(O)(CH_2)_2CHOO: \quad S = 1 - \left[\left(\frac{8}{12} \right) \times 0.95 \times \left(\frac{5}{8+(5-3)} \right) \right] = 0.68 \quad (E6)$$

842

Formatted: Font: 10 pt, Not Bold

Formatted: Font: 10 pt, Not Bold, Not Italic

Deleted: Table 3

Deleted: ¶

¶

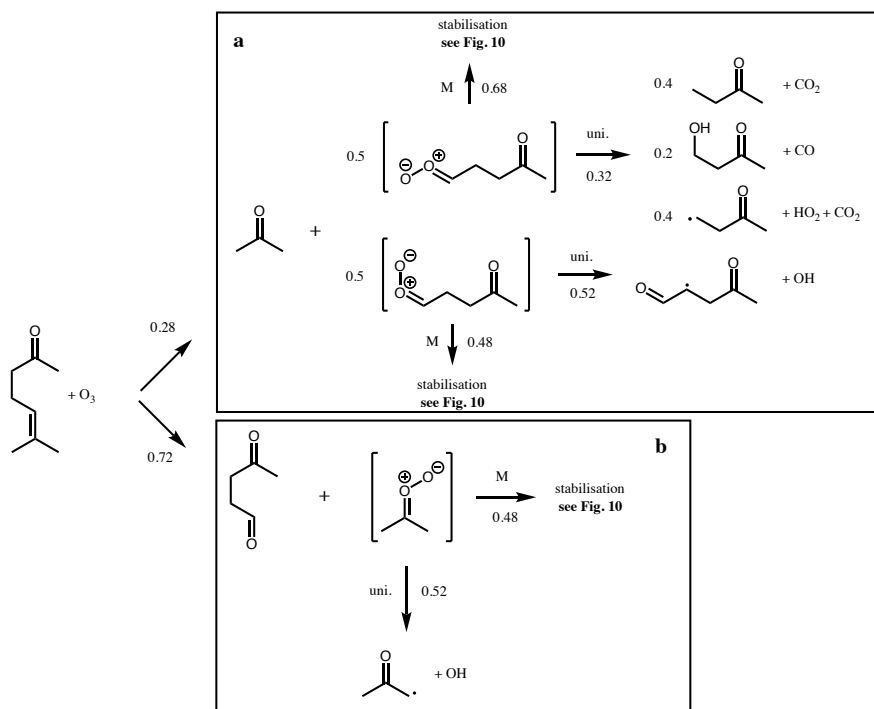
¶

Formatted: Superscript

Deleted: cm³

848 The remaining $(\text{CH}_3)_2\text{COO}^*$ undergoes unimolecular decomposition via the vinylhydroperoxide (VHP) pathway
 849 to yield the acetyl peroxy radical $(\text{CH}_3\text{C}(\text{O})\text{CH}_2\text{OO})$ and OH. The remaining $(Z)\text{-CH}_3\text{C}(\text{O})(\text{CH}_2)_2\text{CHOO}$
 850 decomposes via the VHP pathway to yield $\text{CH}_3\text{C}(\text{O})\text{CH}_2\text{CH}(\text{O}_2)\text{CHO} + \text{OH}$, while $(E)\text{-CH}_3\text{C}(\text{O})(\text{CH}_2)_2\text{CHOO}$
 851 decomposes via 1,3 ring closure and yields $\text{CH}_3\text{C}(\text{O})\text{CH}_2\text{CH}_3 + \text{CO}_2$ (40%), $\text{CH}_3\text{C}(\text{O})\text{CH}_2\text{CH}_2\text{OH} + \text{CO}$ (20%),
 852 $\text{CH}_3\text{C}(\text{O})\text{CH}_2\text{CH}_2 + \text{H} + \text{CO}_2$ (40%). Each stabilised CI can decompose via the same pathways as its respective
 853 CI^* , with temperature dependent rates determined from Vereecken et al. (2017). At 298K these are 478 s^{-1} , 205 s^{-1}
 854 1 and 74 s^{-1} for $(\text{CH}_3)_2\text{COO}$, $(Z)\text{-CH}_3\text{C}(\text{O})(\text{CH}_2)_2\text{CHOO}$ and $(E)\text{-CH}_3\text{C}(\text{O})(\text{CH}_2)_2\text{CHOO}$ respectively.
 855 Alternatively, they can undergo bimolecular reaction. Reaction rates with H_2O and $(\text{H}_2\text{O})_2$ are calculated using
 856 monomer and dimer reaction rates from Vereecken et al. (2017). Reaction rates with other trace gases are taken
 857 from Table 3 for the relevant CI structure. Figure 10 shows calculated pseudo first order reaction rates for reaction
 858 with SO_2 and RCOOH assuming atmospheric mixing ratios of $[\text{SO}_2] = 5 \text{ ppbv}$ and $[\text{RCOOH}] = 5 \text{ ppbv}$.

859



860
861
862

Figure 9. Branching ratios and products of the CI decomposition produced following ozonolysis of 6-methyl-5-hepten-2-one

Formatted: Font: 10 pt, Not Bold

Formatted: Font: 10 pt, Not Bold, Not Italic

Deleted: Table 3

Formatted: Font: 10 pt, Not Bold

Formatted: Font: 10 pt, Not Bold, Not Italic

Deleted: Figure 10

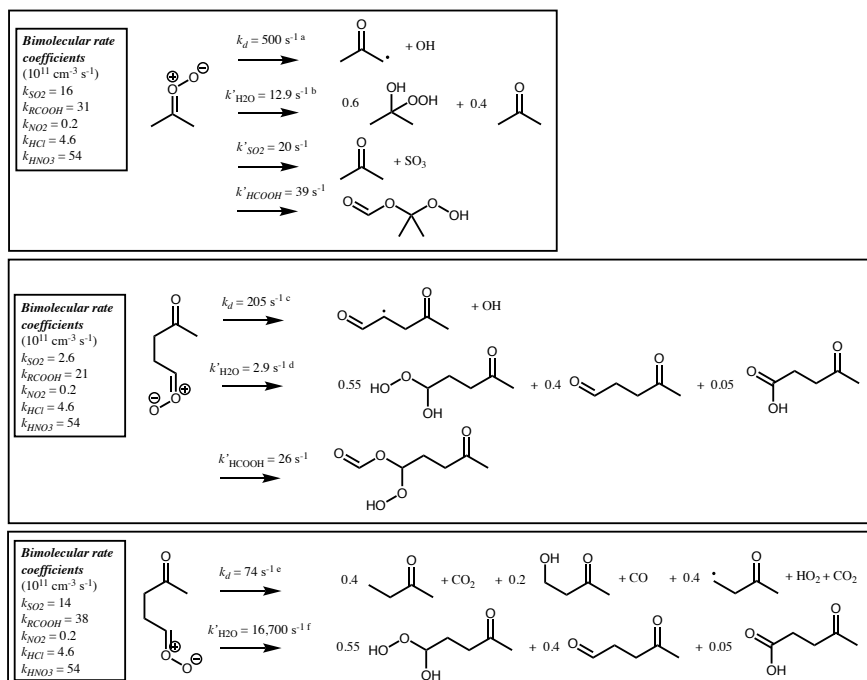


Figure 10. Bimolecular rate coefficients (see Table 3) and products of the SCI produced following ozonolysis of 6-methyl-5-hepten-2-one at 298 K. Pseudo first order loss rates (k^*) and products are shown for decomposition and reaction with water vapour, and for other pathways that contribute more than 1% of the total loss assuming $[\text{SO}_2] = 5 \text{ ppbv}$, $[\text{RCOOH}] = 5 \text{ ppbv}$, $[\text{H}_2\text{O}] = 5 \times 10^{17} \text{ cm}^{-3}$, $[(\text{H}_2\text{O})_2] = 5 \times 10^{14} \text{ cm}^{-3}$, $[\text{NO}_2] = 1 \text{ ppbv}$, $[\text{HCl}] = 100 \text{ pptv}$, $[\text{HNO}_3] = 100 \text{ pptv}$.

^a $7.64 \times 10^{-60} \times T^{23.59} e^{(2367/T)}$

^b Sum of first order loss rates to water monomer ($7.54 \times 10^{-18} * [\text{H}_2\text{O}]$) and dimer ($1.82 \times 10^{-14} * [(\text{H}_2\text{O})_2]$)

^c $2.41 \times 10^{-62} \times T^{24.33} e^{(2571/T)}$

^d Sum of first order loss rates to water monomer ($1.51 \times 10^{-18} * [\text{H}_2\text{O}]$) and dimer ($4.31 \times 10^{-15} * [(\text{H}_2\text{O})_2]$)

^e $1.57 \times 10^{10} \times T^{1.83} e^{(-7464/T)}$

^f Sum of first order loss rates to water monomer ($1.58 \times 10^{-14} * [\text{H}_2\text{O}]$) and dimer ($1.75 \times 10^{-11} * [(\text{H}_2\text{O})_2]$)

878 7 Protocol Evaluation

879 7.1 Experimental databases and assessment approach

880 A database of experimentally determined carbonyl yields, OH yields and SCI yields has been assembled to
 881 evaluate the new protocol (Supplement – Spreadsheets S1-S3). Experimental conditions are also recorded in the
 882 database to enable some assessment of the validity of the assumptions inherent in the experimental setup.

883 The Root Mean Squared Error (RMSE) and the Mean Bias Error (MBE) were examined to assess the
 884 reliability of the protocol. The RMSE and MBE are here defined as:

885

$$886 \text{RMSE} = \sqrt{\frac{1}{n} \sum_{i=1}^n (Y_{\text{protocol}} - Y_{\text{database}})^2} \quad (\text{E7})$$

Deleted: in order

$$888 \quad MBE = \frac{1}{n} \sum_{i=1}^n (Y_{protocol} - Y_{database}) \quad (E8)$$

889 where n is the number of species in the dataset. The databases were split in to subsets to identify possible bias
 890 within a structural category of species (e.g. exocyclic vs endocyclic monoalkenes). The various subsets examined
 891 and their corresponding number of species are summarized in [Table 4](#). Three databases were used to perform the
 892 protocol assessment: carbonyl yields (Spreadsheet S1), SCI yield (S2), and OH yield (S3). The RMSE and MBE
 893 computed for the full databases and the various subsets are reported in [Table 4](#). The scatter plots of protocol yields
 894 vs database yields, by species category, are given in [Figure 11](#).

896 **Table 4. Number of species (n) in the database used to compute the mean bias error (MBE) and the root mean square
 897 error (RMSE) for the OH yields, SCI yields and "longest" carbonyl yield.**

	all species	acyclic monoalkene	endocyclic monoalkene	exocyclic monoalkene	poly alkene	aromatic alkene	oxygenated alkene
<i>OH yields</i>							
n	46	18	8	3	10	3	4
MBE	0.02	-0.01	-0.03	-0.01	0.13	0.03	0.01
RMSE	0.13	0.06	0.09	0.12	0.23	0.09	0.16
<i>SCI yields</i>							
n	22	11	5	2	3	1	0
MBE	0.05	0.02	-0.01	0.22	0.01	0.45	-
RMSE	0.12	0.04	0.04	0.22	0.06	0.45	-
<i>Yields of the longest carbonyl</i>							
n	73	35	NA [‡]	5	5	1	27
MBE	-0.01	-0.02	-	-0.04	0.03	-0.02	0.00
RMSE	0.14	0.11	-	0.12	0.07	0.02	0.18

898 [‡] Endocyclic alkenes do not produce a stable primary carbonyl as all possible molecules formed from the POZ fragmentation
 899 contain a carbonyl oxide moiety.
 900
 901

Deleted: Table 4

Formatted: Font: 10 pt, Not Bold

Deleted: Table 4

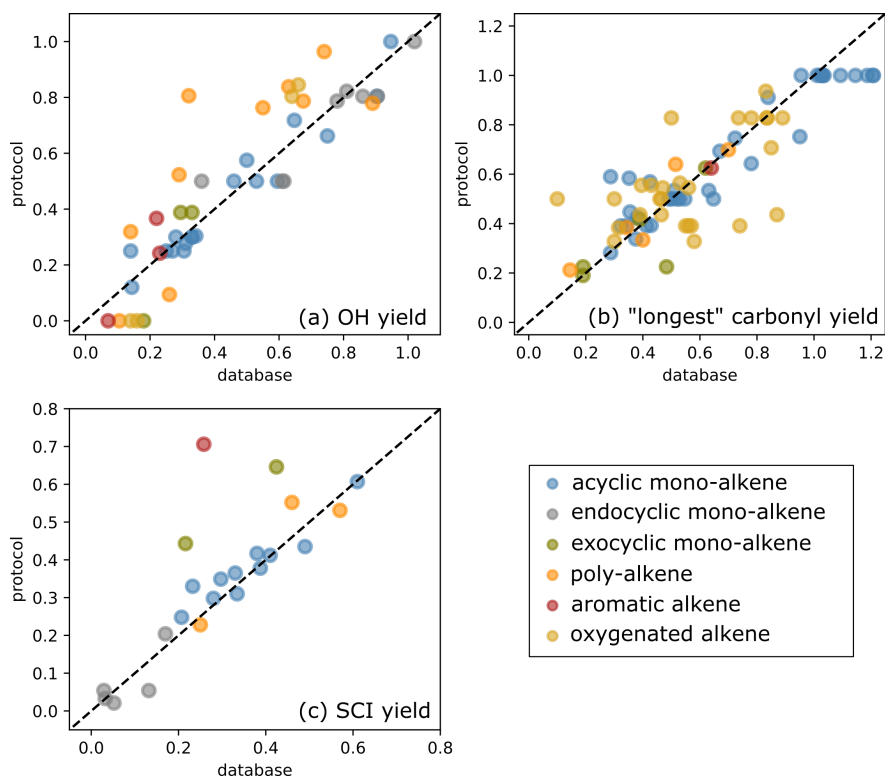
Formatted: Font: 10 pt, Not Bold

Deleted:

Formatted: Font: 10 pt, Not Bold, Font colour: Black

Formatted: Font: 10 pt, Not Bold, Not Italic, Font colour: Black

Deleted: Figure 11



906
907 **Figure 11. Scatter plot of protocol yields vs database yields: (a) OH yields, (b) yields for the "longest" carbonyl and (c)**
908 **SCI yields.**

909 7.2 Primary Carbonyl Yields

910 The primary carbonyl yields from alkene ozonolysis are calculated in the protocol by assigning F values to
911 different functional groups adjacent to the C=C bond that determine the relative fragmentation pattern of the POZ
912 (Section 2). The calculated primary carbonyl yields can be compared to the measurements in the experimental
913 database. For some functional groups however, the number of data available is sparse and the carbonyl yields
914 have been directly used to determine the F value. The carbonyl yields dataset should therefore rather be viewed
915 as a training dataset than a validation dataset in this protocol assessment. [Figure 11b](#) shows the scatter plots for
916 the calculated yields of the larger primary carbonyl (i.e. greater number of non-H atoms) formed in POZ
917 decomposition, compared to the experimentally reported values for each alkene in the database. No substantial
918 bias is identified in the computed carbonyl yields (MBE=-0.01). For non-oxygenated alkenes, the fit is reasonably
919 good and the RMSE does not exceed 0.12 for the various hydrocarbon classes reported in Table 4. The major
920 outlier is the yield of 4-ethyl-3-hexanone from 3,4-diethyl-2-hexene ozonolysis. This is based on one measurement
921 (Grosjean and Grosjean, 1996a). It was noted in Jenkin et al. (2020) that the ozonolysis reaction rate reported by
922 Grosjean and Grosjean (1996b) for this precursor compound is also a significant outlier from predicted trends,
923 and so it seems possible that this compound was incorrectly identified in the original work. For symmetrical

Formatted: Font: 10 pt, Not Bold, Font colour: Black

Deleted: Figure 11

Formatted: Font: 10 pt, Not Bold, Not Italic, Font colour: Black

Deleted: 3-methyl-2-pentanone

Deleted: 7

Deleted: 7

Deleted: was

929 alkenes, the calculated primary carbonyl yield is unity, whereas measured yields tend to cluster slightly above
930 one. This is likely due to a small amount of secondary formation of the carbonyls from bimolecular reactions of
931 SCI. The poorest fitted class is oxygenated alkenes (RMSE=0.18). This is likely due to a combination of factors.
932 Firstly, the majority of these compounds have only one measurement. Secondly, measurements of multi-
933 oxygenated VOCs are known to be more challenging than e.g. simple carbonyls. Thirdly, there is more likely to
934 be additional chemical factors which are not yet understood in the ozonolysis of these more complex molecules
935 influencing the POZ fragmentation. Two of the most significant outliers in the oxygenated alkenes are acrylic and
936 methacrylic acid. As described in Section 2.2.3 it is difficult to reconcile the two available data points.

937 7.3 SCI yields

938 The yield of stabilised Criegee intermediates from an alkene-ozone reaction depends on the alkene structure (i.e.
939 the POZ fragmentation pattern, Section 2), the dominant unimolecular decomposition route of the CI* (Section
940 3.2), and the size of the CI (Section 3.2). The yields calculated by the protocol are independent of the
941 measurements in the database. SCI yields can therefore be considered as a validation dataset to evaluate the
942 reliability of the protocol. Total SCI yields have been measured for a number of alkenes, although the dataset is
943 still relatively small. It should also be noted that many experimentally determined SCI yields have a large
944 uncertainty associated with them, particularly earlier experiments where analysis techniques were less developed
945 and the chemical models lacking. [Figure 11c](#) shows the scatter plot of the total SCI yields calculated by the
946 protocol vs experimental data. The data consists predominantly of acyclic monoalkenes, for which there is a good
947 agreement between the measurements and the calculated values (RMSE=0.04). [Figure 11c](#) shows three major
948 outliers for which the protocol over-predicts the measured SCI yield. These species are methylene cyclohexane
949 and β -pinene (which constitute the subset of the exocyclic alkenes (RMSE=0.22)) and styrene, the only
950 representative of the aromatic alkenes class in this dataset (RMSE=0.45). The methylene cyclohexane and styrene
951 values are both based on one measurement (Hatakeyama et al., 1984), and the β -pinene value is based on two
952 measurements (Hatakeyama et al., 1984; Newland et al., 2018) which are in poor agreement, giving values of 0.25
953 and 0.60 respectively. This clearly warrants revisiting experimentally, particularly with respect to the
954 atmospherically important monoterpene β -pinene. Finally, the overall protocol SCI yields appear to be biased
955 slightly high (+ 5%), which is mainly explained by the overestimation described above for the exocyclic and
956 aromatic alkenes.

957 7.4 OH yields

958 The reaction of alkenes with ozone yields OH through both primary (i.e. decomposition of CI via a
959 vinylhydroperoxide) and secondary (i.e. peroxy radical chemistry) processes. The primary process can also be
960 split: the decomposition of chemically activated CI*, which under atmospheric conditions (and e.g. chamber
961 laboratory experiment conditions) is assumed to happen at rates such that there is no competition with bimolecular
962 reaction; and the decomposition of stabilised CI, which occurs in competition with bimolecular reactions so that
963 the OH yield depends on the unimolecular rate relative to the concentrations of possible co-reactants. The primary
964 OH yield thus depends on the POZ fragmentation pattern (Section 2) and the decomposition pathways of the CI
965 (Section 3.2).

Formatted: Font: 10 pt, Not Bold, Font colour: Black

Formatted: Font: 10 pt, Not Bold, Not Italic, Font colour: Black

Deleted: Figure 11

Formatted: Font: 10 pt, Not Bold, Font colour: Black

Formatted: Font: 10 pt, Not Bold, Not Italic, Font colour: Black

Deleted: Figure 11

968 Many studies have measured the OH yield for specific alkene-ozone reactions. As for the SCI yields
969 above, the OH yield database can be viewed as a validation dataset to assess the reliability of the protocol since
970 OH yields are not prescribed explicitly, but are a product of the protocol rules for POZ fragmentation and CI
971 decomposition pathways. For the comparison, protocol yields are computed assuming that all SCI produced
972 undergo unimolecular decomposition (i.e. bimolecular reactions of SCI are ignored). Although many experiments
973 will have been designed in such a way as to try to prevent bimolecular reactions, in reality a small fraction of the
974 SCI will react bimolecularly, not producing OH, so the computed OH yield might be considered an upper limit.
975 On the other hand, in many of the experiments there will likely be some contribution to the measured OH yield
976 from peroxy radical chemistry (e.g. HO₂ + O₃), making the reported experimental yield an upper limit. No attempt
977 is made here to determine the relative contribution from primary or secondary processes in the reported
978 measurements, which is dependent on both experimental setup and the particular alkene being studied, or to
979 correct for possible bimolecular reactions. Therefore, a comparison between experimental and protocol OH yields
980 clearly carries significant uncertainties.

981 With this in mind, the agreement between computed OH yields and the experimental values is very good
982 (Figure 11a). No substantial bias is observed on the complete dataset (MBE=0.02). It is difficult to comment on
983 some classes as they contain only one or two compounds (see Table 4). The protocol appears especially reliable
984 for estimating the OH yields for monoalkenes (RMSE=0.06) and endocyclic alkenes (RMSE=0.09). The class for
985 which the protocol does worst is polyalkenes (RMSE=0.23), with a systematic over-prediction at higher OH yields
986 (MBE=0.13). There are five compounds for which the protocol calculates an OH yield of zero (styrene, 1,3-
987 butadiene, methyl vinyl ketone, methacrolein, and camphene). The measured OH yields of these compounds are
988 all below 0.2 and the measured OH could be a result of peroxy radical chemistry.

989 8 Conclusions

990 This manuscript provides a protocol by which the central features of alkene ozonolysis chemistry can be included
991 in an explicit automatic chemical mechanism generator. It also serves to highlight the many gaps that remain in
992 our knowledge of this complex, atmospherically important, process. This will hopefully help direct both
993 experimental and theoretical research towards improving understanding in these areas. Some of the major areas
994 of uncertainty identified in this work include:

- 996 (i) The impact of oxygenated substituents on POZ fragmentation
- 997 (ii) The impact of alkene structure on (*E*)/(*Z*)-CI conformer yields
- 998 (iii) Products of the hot acid / ester channel and trends in the stabilisation of the hot acid / ester with size
- 999 (iv) Further details of the mechanisms and products of non-Criegee ozonolysis chemistry, e.g. step-wise
1000 decomposition of the POZ via a carbonyl hydroperoxide
- 1001 (v) Product distributions of some of the major atmospheric SCI bimolecular reactions – e.g. the reaction
1002 of (*Z*)-RCHO / CH₂OO with H₂O / (H₂O)₂
- 1003 (vi) Experimental evidence of the products of conjugated alkene ozonolysis
- 1004 (vii) Data on OH and SCI yields from alkenes with (multiple) functional groups

1005 The reliability of the protocol designed in this work was assessed using experimental values for the OH, SCI and
1006 primary carbonyl yields, which are independent of the data used to derive the protocol. For these three datasets,
1007

Formatted: Font: 10 pt, Not Bold, Font colour: Black

Formatted: Font: 10 pt, Not Bold, Not Italic, Font colour: Black

Deleted: Figure 11

1009 the Mean Bias Error (MBE) for the protocol based yields is below 0.05, with no substantial bias identified. The
1010 protocol currently provides a fairly reliable estimate of the OH, SCI and primary carbonyl yields with Root Mean
1011 Squared Errors (RMSE) of 0.12, 0.13 and 0.15, respectively. [The protocol thus appears robust in representing CI](#)
1012 [chemistry and its impact on atmospheric chemistry](#). However, the number of data available for some classes of
1013 compounds remains limited, such as oxygenated, exocyclic and poly-alkenes. The errors in the yields calculated
1014 for these species are also the most substantial, and additional experimental data for these categories of compound
1015 would be highly valuable to improve the protocol and its assessment.

1016 **Acknowledgements**

1017 This work was performed as part of the MAGNIFY project, with funding from the French National Research Agency (ANR)
1018 under project ANR-14-CE01-0010, and the UK Natural Environment Research Council (NERC) via grant NE/M013448/1. It
1019 was also partially funded by the European Commission (EUROCHAMP-2020 (grant no. 730997)) and the UK National Centre
1020 for Atmospheric Sciences (NCAS) Air Pollution Theme.

1021 **Data availability**

1022 [All relevant data and supporting information have been provided in the Supplement.](#)

1023 **Author contribution**

1024 [All authors defined the scope of the work. MJN and CM-V developed and applied the SAR methods with the help of LV,](#)
1025 [which were reviewed by all co-authors. MJN drafted the manuscript with the help of ARR, which was reviewed by all co-](#)
1026 [authors. RV and BA tested the SAR methods in GECKO-A and carried out the statistical analysis in Section 7.](#)

1027 **Competing interests**

1028 [The authors declare that they have no conflict of interest.](#)

1029 **Special issue statement**

1030 This article is part of the special issue "Simulation chambers as tools in atmospheric research (AMT/ACP/GMD inter-journal
1031 SD)". It is not associated with a conference.

1032 **References**

- 1033 Ahrens, J., Carlsson, P. T. M., Hertl, N., Olzmann, M., Pfeifle, M., Wolf, J. L., and Zeuch, T.: Infrared Detection of Criegee
1034 Intermediates Formed during the Ozonolysis of β -pinene and Their Reactivity towards Sulfur Dioxide, *Angew. Chem.*, 53,
1035 715–719, 2014.
- 1036 Alam, M. S., Camredon, M., Rickard, A. R., Carr, T., Wyche, K. P., Hornsby, K. E., Monks, P. S., and Bloss, W. J.: Total
1037 radical yields from tropospheric ethene ozonolysis, *Phys. Chem. Chem. Phys.*, 13, 11002–11015, 2011.
- 1038 Almatarneh, M. H., Elayan, I. A., Altarawneh, M., and Hollett, J. W.: A computational study of the ozonolysis of sabinene,
1039 *Theor. Chem. Acc.*, 138, Article No. 30, 2019.
- 1040 Al Mulla, I., Viera, L., Morris, R., Sidebottom, H., Treacy, J., and Mellouki, A.: Kinetics and Mechanisms for the Reactions
1041 of Ozone with Unsaturated Oxygenated Compounds, *Chem. Phys. Chem.*, 11, 4069–4078, 2010.
- 1042 Anglada, J. M., Bofill, J. M., Olivella, S., and Solé, A.: Theoretical Investigation of the Low-Lying Electronic States of
1043 Dioxirane: Ring Opening to Dioxymethane and Dissociation into CO₂ and H₂, *J. Phys. Chem. A*, 102, 3398–3406, 1998.

1044 Anglada, J. M., Crehuet, R., and Bofill, J. M.: The Ozonolysis of Ethylene: A Theoretical Study of the Gas-Phase Reaction
1045 Mechanism, *Chem. Eur. J.*, 5, 1809-1822, 1999.

1046 Aschmann, S. M., Tuazon, E. C., Arey, J., and Atkinson, R.: Products of the Gas-Phase Reaction of O₃ with Cyclohexene, *J.*
1047 *Phys. Chem. A*, 107, 2247–2255, 2003.

1048 Atkinson, R., and Aschmann, S. M.: OH radical production from the gas-phase reactions of O₃ with a series of alkenes under
1049 atmospheric conditions, *Environ. Sci. Technol.*, 27, 1357-1363, 1993.

1050 Atkinson, R., Baulch, D. L., Cox, R. A., Crowley, J. N., Hampson, R. F., Hynes, R. G., Jenkin, M. E., Rossi, M. J., Troe, J.,
1051 and IUPAC Subcommittee: Evaluated kinetic and photochemical data for atmospheric chemistry: Volume II – gas phase
1052 reactions of organic species, *Atmos. Chem. Phys.*, 6, 3625–4055, <https://doi.org/10.5194/acp-6-3625-2006>, 2006.

1053 Aumont, B., Szopa, S., and Madronich, S.: Modelling the evolution of organic carbon during its gas-phase tropospheric
1054 oxidation: development of an explicit model based on a self generating approach, *Atmos. Chem. Phys.*, 5, 2497-2517,
1055 <https://doi.org/10.5194/acp-5-2497-2005>, 2005.

1056 Barber, V. P., Shubhrangshu, P., Green, A. M., Trongsiwat, N., Walsh, P. J., Klippenstein, S. J., and Lester, M. I.: Four-
1057 Carbon Criegee Intermediate from Isoprene Ozonolysis: Methyl Vinyl Ketone Oxide Synthesis, Infrared Spectrum, and OH
1058 Production, *J. Am. Chem. Soc.*, 140, 10866-10880, 2018.

1059 Barber, V. P., Hansen, A. S., Georgievskii, Y., Klippenstein, S. J., and Lester, M. I.: Experimental and theoretical studies of
1060 the doubly substituted methyl-ethyl Criegee intermediate : Infra-red action spectroscopy a unimolecular decay to OH radical
1061 products, *J. Chem. Phys.*, 152, 094301, doi:10.1063/5.0002422, 2020.

1062 Barnes, I., Zhou, S.M., Klotz, B.: In Final Report of the EU project MOST, Contract EVK2-CT-2001-00114. European Union,
1063 Brussels, 2005.

1064 Bauld, N. L., Thompson, J. A., Hudson, C. E., and Bailey, P. S.: Stereospecificity in Ozonide and Cross-Ozonide Formation,
1065 *J. Am. Chem. Soc.*, 90, 1822-1830, 1968.

1066 Bernard, F., Eyglunet, G., Daële, V., and Mellouki, A.: Kinetics and Products of Gas-Phase Reactions of Ozone with Methyl
1067 Methacrylate, Methyl Acrylate, and Ethyl Acrylate, *J. Phys. Chem. A*, 114, 8376–8383, 2010.

1068 Berndt, T., Voigtländer, J., Stratmann, F., Junninen, H., Mauldin III, R. L., Sipilä, M., Kulmala, M., and Herrmann, H.:
1069 Competing atmospheric reactions of CH₂OO with SO₂ and water vapour, *Phys. Chem. Chem. Phys.*, 16, 19130–19136, 2014a.

1070 Berndt, T., Jokinen, T., Sipilä, M., Mauldin III, R. L., Herrmann, H., Stratmann, F., Junninen, H., and Kulmala, M.: H₂SO₄
1071 formation from the gas-phase reaction of stabilized Criegee intermediates with SO₂: Influence of water vapour content and
1072 temperature, *Atmos. Environ.*, 89, 603-612, 2014b.

1073 Berndt, T., Kaethner, R., Voigtländer, J., Stratmann, F., Pfeifle, M., Reichle, P., Sipilä, M., Kulmala, M., and Olzmann, M.:
1074 Kinetics of the unimolecular reaction of CH₂OO and the bimolecular reactions with the water monomer, acetaldehyde and
1075 acetone under atmospheric conditions, *Phys. Chem. Chem. Phys.*, 17, 19862–19873, 2015.

1076 Bey, I., Aumont, B., and Toupance, G: The nighttime production of OH radicals in the continental troposphere, *Geophys. Res.*
1077 *Letts*, 24, 1067-1070, 1997.

1078 Cabezas, C., and Endo, Y.: Spectroscopic Characterization of the Reaction Products between the Criegee Intermediate CH₂OO
1079 and HCl, *Chem. Phys. Chem.*, 18, 1860-1863, 2017.

1080 Cabezas, C., and Endo, Y.: The reaction between the methyl Criegee intermediate and hydrogen chloride: an FTMW spectroscopic
1081 study, *Phys. Chem. Chem. Phys.*, 20, 22569-22575, 2018.

1082 Cabezas, C., and Endo, Y.: Observation of hydroperoxyethyl formate from the reaction between the methyl Criegee intermediate and
1083 formic acid, *Phys. Chem. Chem. Phys.*, 22, 446-454, 2020.

1084 Calvert, J. G., Atkinson, R., Kerr, J. A., Madronich, S., Moortgat, G. K., Wallington, T. J., and Yarwood, G.: The Mechanism of
1085 Atmospheric Oxidation of the Alkenes, Oxford University Press, New York, USA, 552 pp., 2000.

1086 Campos-Pineda, M. and Zhang, J.: Product yields of stabilized Criegee intermediates in the ozonolysis reactions of *cis*-2-
1087 butene, 2-methyl-2-butene, cyclopentene, and cyclohexene, *Science China Chemistry*, 61, 850-856, 2018.

1088 Caravan, R. L., Khan, A. H. M., Rotavera, B., Papajak, E., Antonov, I. O., Chen, M. -W., Au, K., Chao, W., Osborn, D. L.,
1089 Lin, J. J. -M., Percival, C. J., Shallcross, D. E., and Taatjes, C. E.: Products of Criegee intermediate reactions with NO₂:
1090 experimental measurements and tropospheric implications, *Faraday Discuss.*, 200, 313-330, 2017.

1091 Caravan, R. L., Vansco, M. F., Au, K., Khan, M. A. H., Li, Y. L., Winiberg, F. A., ... & Lester, M. I.: Direct kinetic
1092 measurements and theoretical predictions of an isoprene-derived Criegee intermediate. *Proceedings of the National Academy
1093 of Sciences*, 117(18), 9733-9740, 2020.

1094 Carr, S. A., Glowacki, D. R., Liang, C. -H., Baeza-Romero, M. T., Blitz, M. A., Pilling, M. J., and Seakins, P. W.: Experimental
1095 and Modeling Studies of the Pressure and Temperature Dependences of the Kinetics and the OH Yields in the Acetyl + O₂
1096 Reaction, *J. Phys. Chem. A*, 115, 1069–1085, 2011.

1097 Carlaw, N.: A new detailed chemical model for indoor air pollution, *Atmos. Environ.*, 41, 1164-1179, 2007.

1098 Chang, J. -G., Chen, H. -T., Xu, S., and Lin, M. C.: Computational study on the kinetics and mechanisms for the unimolecular
1099 decomposition of formic and oxalic acids, *J. Phys. Chem. A*, 111, 6789–6797, 2007.

1100 Chao, W., Hsieh, J. -T., Chang C.-H., and Lin J. J. -M.: Direct kinetic measurement of the reaction of the simplest Criegee
1101 intermediate with water vapour, *Science*, 347, 751–754, doi:10.1126/science.1261549, 2015.

1102 Chen, B. -Z., Anglada, J. M., Huang, M. -B., and Kong, F.: The Reaction of CH₂ (X³B₁) with O₂ (X³Σ_g⁻): A Theoretical
1103 CASSCF/CASPT2 Investigation, *J. Phys. Chem. A*, 106, 1877–1884, 2002.

1104 Chhantyal-Pun, R., Davey, A., Shallcross, D. E., Percival, C. J., and Orr-Ewing, A. J.: A kinetic study of the CH₂OO Criegee
1105 intermediate self-reaction, reaction with SO₂ and unimolecular reaction using cavity ring-down spectroscopy, *Phys. Chem.
1106 Chem. Phys.*, 17, 3617–3626, 2015.

1107 Chhantyal-Pun, R., Khan, M. A. H., Taatjes, C. A., Percival, C. J., Orr-Ewing, A. J., and Shallcross, D. E.: Criegee
1108 intermediates: production, detection and reactivity, *Int. Rev. Phys. Chem.*, 39, 385-424, 2020.

1109 Chung, C. -A., Su, J. W., and Lee, Y. -P.: Detailed mechanism and kinetics of the reaction of Criegee intermediate CH₂OO
1110 with HCOOH investigated *via* infrared identification of conformers of hydroperoxymethyl formate and formic acid anhydride,
1111 *Phys. Chem. Chem. Phys.*, 21, 21445–21455, 2019.

1112 Chuong, B., Zhang, J., and Donahue, N. M.: Cycloalkene Ozonolysis: Collisionally Mediated Mechanistic Branching, *J. Am.
1113 Chem. Soc.*, 126, 12363–12373, 2004.

1114 Cremer, D.: Stereochemistry of the Ozonolysis of Alkenes: Ozonide versus Carbonyl Oxide Control, *Angew. Chem.*, 20,
1115 888-889, 1981.

1116 Cox, R. A., Ammann, M., Crowley, J. N., Herrmann, H., Jenkin, M. E., McNeill, V. F., Mellouki, A., Troe, J., and Wallington,
1117 T. J.: Evaluated kinetic and photochemical data for atmospheric chemistry: Volume VII – Criegee intermediates, *Atmos.
1118 Chem. Phys.*, 20, 13497-13519, 2020.

1119 Cremer, D.: Theoretical Determination of Molecular Structure and Conformation. 8. Energetics of the Ozonolysis Reaction.
1120 Primary Ozonide vs. Carbonyl Oxide Control of Stereochemistry, *J. Am. Chem. Soc.*, 103, 3627-3633, 1981.

1121 Drozd, G. T., Kroll, J., and Donahue, N. M.: 2,3-Dimethyl-2-butene (TME) ozonolysis: Pressure dependence of stabilized
1122 criegee intermediates and evidence of stabilized vinyl hydroperoxides, *J. Phys. Chem. A*, 115, 161-166, 2011.

1123 Drozd, G. T., and Donahue, N. M.: Pressure dependence of stabilized Criegee intermediate formation from a sequence of
1124 alkenes, *J. Phys. Chem. A*, 115, 4381-4387, 2011.

1125 Drozd, G. T., Kurtén, T., Donahue, N. M., Lester, M. I.: Unimolecular decay of the dimethyl-substituted criegee intermediate
1126 in alkene ozonolysis: Decay time scales and the importance of tunnelling, *J. Phys. Chem. A*, 121, 6036-6045, 2017.

1127 Ehn, M., Thornton, J. A., Kleist, E., Sipilä, M., Junninen, H., Pullinen, I., Springer, M., Rubach, F., Tillmann, R., Lee, B.,
1128 Lopez-Hilfiker, F., Andres, S., Acir, I.-H., Rissanen, M., Jokinen, T., Schobesberger, S., Kangasluoma, J., Kontkanen, J.,
1129 Nieminen, T., Kurtein, T., Nielsen, L. B., Jørgensen, S., Kjaergaard, H. G., Canagaratna, M., Maso, M. D., Berndt, T., Petäjä,
1130 T., Wahner, A., Kerminen, V.-M., Kulmala, M., Worsnop, D. R., Wildt, J., and Mentel, T. F.: A large source of low-volatility
1131 secondary organic aerosol, *Nature*, 506, 476–479, <https://doi.org/10.1038/nature13032>, 2014.

1132 Elshorbany, Y. F., Kurtenbach, R., Wiesen, P., Lissi, E., Rubio, M., Villena, G., Gramsch, E., Rickard, A. R., Pilling, M. J.,
1133 and Kleffmann, J.: Oxidation capacity of the city air of Santiago, Chile, *Atmos. Chem. Phys.*, 9, 2257–2273,
1134 <https://doi.org/10.5194/acp-9-2257-2009>, 2009.

1135 Emmerson, K. M., Carslaw, N., and Pilling, M. J.: Urban Atmospheric Chemistry During the PUMA Campaign 2: Radical
1136 Budgets for OH, HO₂ and RO₂, *J. Atmos. Chem.*, 52, 165-183, 2005.

1137 Fenske, J. D., Hasson, A. S., Paulson, S. E., Kuwata, K. T., Ho, A., and Houk, K. N.: The Pressure Dependence of the OH
1138 Radical Yield from Ozone-Alkene Reactions, *J. Phys. Chem. A*, 104, 7821-7833, 2000.

1139 Fliszár, S., and Granger, M.: A Quantitative Investigation of the Ozonolysis Reaction: XI. On the Effects of Substituents in
1140 Directing the Ozone Cleavage of trans-1,2-Disubstituted Ethylenes, *J. Am. Chem. Soc.*, 92, 3361-3369, 1970.

1141 Fliszár, S., and J., Renard: Quantitative investigation of the ozonolysis reaction. XIV. A simple carbonium ion stabilization
1142 approach to the ozone cleavage of unsymmetrical olefins, *J. Am. Chem. Soc.*, 93, 6953-6963, 1970.

1143 Fliszár, S., J., Renard, and Simon, D. Z.: A Quantitative Investigation of the Ozonolysis Reaction. XV. Quantum Chemical
1144 Interpretation of the Substituent Effects on the Cleavage of 1,2,3-Trioxolanes, *J. Am. Chem. Soc.*, 93, 6953-6963, 1971.

1145 Foreman, E. S., Kapnas, K. M., and Murray, C.: Reactions between Criegee Intermediates and the inorganic Acids HCl and
1146 HNO₃: Kinetics and Atmospheric Implications, *Angew. Chem. Int. Ed. Engl.*, 55, doi:10.1002/anie.201604662, 2016.

1147 Grosjean, D., Williams, E. L., and Grosjean, E.: Atmospheric chemistry of isoprene and of its carbonyl products, *Environ. Sci.*
1148 *Technol.*, 27, 830–840, 1993.

1149 Grosjean, D., Williams, E. L., Grosjean, E., Andino, J. M., and Seinfeld, J. H.: Atmospheric oxidation of biogenic
1150 hydrocarbons: reaction of ozone with β -pinene, d-limonene and trans-caryophyllene, *Environ. Sci. Technol.*, 27, 2754–2758,
1151 1993.

1152 Grosjean, D., Grosjean, E., and Williams, E. L.: Atmospheric Chemistry of Olefins: A Product Study of the Ozone-Alkene
1153 Reaction with Cyclohexane Added to Scavenge OH, *Environ. Sci. Technol.*, 28, 188–196, 1994.

1154 Grosjean, E., Grosjean, D., and Seinfeld, J. H.: Gas phase reaction of ozone with trans-2-hexenal, trans-2-hexenyl acetate,
1155 ethylvinyl ketone and 6-methyl-5-hepten-2-one, *Int. J. Chem. Kinet.*, 28, 373–382, 1996.

1156 [Grosjean, E., and Grosjean, D.: Carbonyl products of the gas phase reaction of ozone with 1,1-disubstituted alkenes. *J. Atmos.*
1157 *Chem.*, 24, 141–156. <https://doi.org/10.1007/BF00162408>, 1996a.](#)

1158 [Grosjean, E. and Grosjean, D.: Rate constants for the gas phase reaction of ozone with 1,1-disubstituted alkenes. *Int. J. Chem.*
1159 *Kinet.*, 28, 911–918, 1996b.](#)

1160 [Grosjean, E. and Grosjean, D.: Gas phase reaction of alkenes with ozone: Formation yields of primary carbonyls and
1161 biradicals. *Environ. Sci. Technol.*, 31\(8\), 2421-2427, 1997a.](#)

1162 Grosjean, E., and Grosjean, D.: The Gas Phase Reaction of Unsaturated Oxygenates with Ozone: Carbonyl Products and
1163 Comparison with the Alkene-Ozone Reaction, *J. Atmos. Chem.*, 27, 271-289, 1997b.

1164 Grosjean, E., and Grosjean, D.: The Reaction of Unsaturated Aliphatic Oxygenates with Ozone, *J. Atmos. Chem.*, 32, 205-
1165 232, 1999.

1166 Gutbrod, R., Meyer, S., Rahman, M. M., and Schindler, R. N.: On the use of CO as scavenger for OH radicals in the ozonolysis
1167 of simple alkenes and isoprene, *Int. J. Chem. Kinet.*, 29, 717-723, 1997.

1168 Hakala, J. P., and Donahue, N. M.: Pressure-Dependent Criegee Intermediate Stabilization from Alkene Ozonolysis, *J. Phys.*
1169 *Chem. A*, 120, 2173-2178, 2016.

1170 Hakala, J. P., and Donahue, N. M.: Pressure Stabilization of Criegee Intermediates Formed from Symmetric trans-Alkene
1171 Ozonolysis, *J. Phys. Chem. A*, 122, 9426-9434, 2018.

1172 Hakola, H., Arey, J., Aschmann, S. M., and Atkinson, R.: Product formation from the gas-phase reactions of OH radicals and
1173 O₃ with a series of monoterpenes, *J. Atmos. Chem.*, 18, 75-102, 1994.

1174 [Hansel, A., Scholz, W., Mentler, B., Fischer, L., and Berndt, T.: Detection of RO₂ radicals and other products from
1175 cyclohexene ozonolysis with NH₄⁺ and acetate chemical ionization mass spectrometry. *Atmospheric Environment*, 186, 248-
1176 255, <https://doi.org/10.1016/j.atmosenv.2018.04.023>, 2018.](#)

1177 Hasson, A. S., Orzechowska, G., and Paulson, S. E.: Production of stabilized Criegee intermediates and peroxides in the gas
1178 phase ozonolysis of alkenes 1. Ethene, trans-2-butene, and 2,3- dimethyl-2-butene, *J. Geophys. Res.*, 106, 34131–34142,
1179 2001a.

1180 Hasson, A. S., Ho, A. W., Kuwata, K., and Paulson, S. E.: Production of stabilized Criegee intermediates and peroxides in the
1181 gas phase ozonolysis of alkenes 2. Asymmetric and biogenic alkenes, *J. Geophys. Res.*, 106, 34143–34153, 2001b.

1182 Hatakeyama, S., Kobayashi, H., and Akimoto, H.: Gas-phase oxidation of sulfur dioxide in the ozone-olefin reactions, *J. Phys.*
1183 *Chem.* 88, 4736-4739, 1984.

1184 Heard, D. E., Carpenter, L. J., Creasey, D. J., Hopkins, J. R., Lee, J. R., Lewis, A. C., Pilling, M. J., Seakins, P. W., Carslaw,
1185 N., and Emmerson, K. M.: High levels of the hydroxyl radical in the winter urban troposphere, *Geophys. Res. Lett.*, 31,
1186 L18112, 2004.

1187 Herron, J. T., and Huie, R. E. Stopped-flow studies of the mechanisms of ozone-alkene reactions in the gas phase: propene
1188 and isobutene, *J. Am. Chem. Soc.*, 99, 5430-5435, 1977.

1189 Herron, J. T., and Huie, R. E. Stopped-flow studies of the mechanisms of ozone-alkene reactions in the gas phase. I. Ethylene,
1190 *J. Am. Chem. Soc.*, 99, 5430-5435, 1978.

1191 Huang, H. -L., Chao, W., and Lin, J. J. -M.: Kinetics of a Criegee intermediate that would survive at high humidity and may
1192 oxidize atmospheric SO₂, *Proc. Natl. Acad. Sci.*, 112, 10857–10862, 2015.

1193 Iyer, S., Rissanen, M. P., Valiev, R., Barua, S., Krechmer, J. E., Thornton, J., Ehn, M., and Kurtén, T.: Molecular mechanism
1194 for rapid autoxidation in α -pinene ozonolysis, *Nat. Comms.*, 12, doi.org/10.1038/s41467-021-21172-w, 2021.

1195 Jenkin, M. E., Saunders, S. M., and Pilling, M. J.: The tropospheric degradation of volatile organic compounds: a protocol for
1196 mechanism development, *Atmos. Environ.*, 31, 81–104, 1997.

1197 Jenkin, M. E., Young, J. C., and Rickard, A. R.: The MCM v3.3.1 degradation scheme for isoprene, *Atmos. Chem. Phys.*, 15,
1198 11433-11459, 2015.

1199 Jenkin, M. E., Valorso, R., Aumont, B., Rickard, A. R., and Wallington, T. J.: Estimation of rate coefficients and branching
1200 ratios for gas-phase reactions of OH with aliphatic organic compounds for use in automated mechanism construction, *Atmos.*
1201 *Chem. Phys.*, 18, 9297–9328, <https://doi.org/10.5194/acp-18-9297-2018>, 2018a.

1202 Jenkin, M. E., Valorso, R., Aumont, B., Rickard, A. R., and Wallington, T. J.: Estimation of rate coefficients and branching
1203 ratios for gas-phase reactions of OH with aromatic organic compounds for use in automated mechanism construction, *Atmos.*
1204 *Chem. Phys.*, 18, 9329–9349, <https://doi.org/10.5194/acp-18-9329-2018>, 2018b.

1205 Jenkin, M. E., Valorso, R., Aumont, B., and Rickard, A. R.: Estimation of rate coefficients and branching ratios for reactions
1206 of organic peroxy radicals for use in automated mechanism construction, *Atmos. Chem. Phys.*, 19, 7691–7717,
1207 <https://doi.org/10.5194/acp-19-7691-2019>, 2019.

1208 Jenkin, M. E., Valorso, R., Aumont, B., Newland, M. J., and Rickard, A. R.: Estimation of rate coefficients for the reactions
1209 of O₃ with unsaturated organic compounds for use in automated mechanism construction, *Atmos. Chem. Phys.*, 20, 12921-
1210 12937, 2020.

1211 Johnson, D. and Marston, G.: The gas-phase ozonolysis of unsaturated volatile organic compounds in the troposphere, *Chem.*
1212 *Soc. Rev.*, 37, 699–716, 2008.

1213 Kalalian, C., Roth, E., El Dib, G., Singh, H. J., Rao, P. K., and Chakir, A.: Product investigation of the gas phase ozonolysis
1214 of 1-penten-3-ol, *cis*-2-penten-1-ol and *trans*-3-hexen-1-ol, *Atmos. Environ.*, 238, 117732, 2020.

1215 Kalberer, M., Yu, J., Cocker, D. R., Flagan, R. C., and Seinfeld, J. H.: Aerosol Formation in the Cyclohexene-Ozone System,
1216 *Environ. Sci. Technol.*, 34, 4894-4901, 2000.

1217 Kidwell, N. M., Li, H., Wang, X., Bowman, J. M., and Lester, M. I.: Unimolecular dissociation dynamics of vibrationally
1218 activated CH₃CHOO Criegee intermediates to OH radical products, *Nat. Chem.*, 8, 509-514, 2016.

1219 Klotz, B., Barnes, I., and Imamura, T.: Product study of the gas phase reactions of O₃, OH and NO₃ reactions with methyl
1220 vinyl ether, *Phys. Chem. Chem. Phys.*, 6, 1725–1734, 2004.

1221 Kristensen, K., Cui, T., Zhang, H., Gold, A., Glasius, M., and Surratt, J. D.: Dimers in α -pinene secondary organic aerosol:
1222 effect of hydroxyl radical, ozone, relative humidity and aerosol acidity, *Atmos. Chem. Phys.*, 14, 4201–4218, 2014.

1223 Kroll, J. H., Hanisco, T. F., Donahue, N. M., Demerjian, K. L., and Anderson, J. G.: Accurate, direct measurements of OH
1224 yields from gas-phase ozone-alkene reactions using an in-situ LIF instrument, *Geophys. Res. Lett.*, 28, 3863–3866, 2001.

1225 Kroll, J., Donahue, N. M., Cee, V. J., Demerjian, K. L., and Anderson, J. G.: Gas-phase ozonolysis of alkenes: Formation of
1226 OH from anti carbonyl oxides, *J. Am Chem. Soc.*, 124, 8518–8519, 2002.

1227 Kuwata, K. T., Valin, L. C., and Converse, A. D.: Quantum chemical and master equation studies of the methyl vinyl carbonyl
1228 oxides formed in isoprene ozonolysis, *J. Phys. Chem. A*, 109, 10710–10725, 2005.

1229 Kuwata, K. T., and Valin, L. C.: Quantum chemical and RRKM/master equation studies of isoprene ozonolysis: Methacrolein
1230 and methacrolein oxide, *Chem. Phys. Lett.*, 451, 186–191, 2008.

1231 Kuwata, K. T., Guinn, E. J., Hermes, M. R., Fernandez, J. A., Mathison, J. M., and Huang, K. A.: Computational Re-
1232 examination of the Criegee Intermediate-Sulfur Dioxide Reaction, *J. Phys. Chem. A*, 119, 10316–10335, 2015.

1233 Kuwata, K. T., Luu, L., Weberg, A. B., Huang, K., Parsons, A. J., Peebles, L. A., Rackstraw, N. B., and Kim, M. J.: Quantum
1234 Chemical and Statistical Rate Theory Studies of the Vinyl Hydroperoxides Formed in *trans*-2-Butene and 2,3-Dimethyl-2-
1235 butene Ozonolysis, *J. Phys. Chem. A*, 122, 2485–2502, 2018.

1236 Lee, A., Goldstein, A. H., Keywood, M. D., Gao, S., Varutbangkul, V., Bahreini, R., Ng, N. L., Flagan, R. C., and Seinfeld, J.
1237 H.: Gas-phase products and secondary organic aerosol yields from the ozonolysis of ten different terpenes, *J. Geophys. Res.*,
1238 111, D07302, 2006.

1239 Le Person, A., Solignac, G., Oussar, F., Daële, V., Mellouki A., Winterhalter, R., and Moortgat, G. K.: Gas phase reaction of
1240 allyl alcohol (2-propen-1-ol) with OH radicals and ozone, *Phys. Chem. Chem. Phys.*, 11, 7619–7628, 2009.

1241 [Lei, X., Wang, W., Gao, J., Wang, S. and Wang, W.: Atmospheric Chemistry of Enols: The Formation Mechanisms of Formic
1242 and Peroxyformic Acids in Ozonolysis of Vinyl Alcohol, *J. Phys. Chem. A*, 124, 4271–4279, 2020.](#)

1243 Lewin, A. G., Johnson, D., Price, D. W., and Marston, G.: Aspects of the kinetics and mechanism of the gas-phase reactions
1244 of ozone with conjugated dienes, *Phys. Chem. Chem. Phys.*, 3, 1253–1261, 2001.

1245 Lewis, T. R., Blitz, M. A., Heard, D. E., and Seakins, P. W. Direct evidence for a substantive reaction between the Criegee
1246 intermediate, CH₂OO, and the water vapour dimer, *Phys. Chem. Chem. Phys.*, 17, 4859–4863, 2015.

1247 Lin, L.-C., Chang, H., Chang, C., Chao, W., Smith, M. C., Chang, C., Lin, J. J., and Takahashi, K. Competition between H₂O
1248 and (H₂O)₂ reactions with CH₂OO/CH₃CHOO, *Phys. Chem. Chem. Phys.*, 18, 4557–4568, 2016.

1249 Long, B., Bao, J. L., and Truhlar, D. G.: Rapid unimolecular reaction of stabilized Criegee intermediates and implications for
1250 atmospheric chemistry, *Nat. Commun.*, 10, doi:10.1038/s41467-019-09948-7, 2019.

1251 Ma, Y., and Marston G.: Multifunctional acid formation from the gas-phase ozonolysis of β -pinene, *Phys. Chem. Chem. Phys.*,
1252 10, 6115–6126, 2008.

1253 Ma, Y., and Marston G.: Formation of organic acids from the gas-phase ozonolysis of terpinolene, *Phys. Chem. Chem. Phys.*,
1254 11, 4198–4209, 2009.

1255 Martinez, R. I. and Herron, J. T.: Stopped-flow studies of the mechanisms of alkene-ozone reactions in the gas-phase:
1256 tetramethylethylene, *J. Phys. Chem. A*, 91, 946–953, 1987.

1257 [Mauldin III, R. L., Berndt, T., Sipilä, M., Paasonen, P., Petäjä, T., Kim, S., Kurtén, T., Stratmann, F., Kerminen, V.-M., and
1258 Kulmala, M.: A new atmospherically relevant oxidant of sulphur dioxide, *Nature*, 488, 193–196, doi:10.1038/nature11278,
1259 2012.](#)

1260 Neeb, P., Horie, O., and Moortgat, G. K. The nature of the transitory product in the gas-phase ozonolysis of ethene, *Chem.*
1261 *Phys. Lett.*, 37, 150–156, 1995.

1262 Neeb, P., Horie, O., and Moortgat, G. K. Formation of secondary ozonides in the gas-phase ozonolysis of simple alkenes,
1263 *Tetrahedron Lett.*, 246, 9297–9300, 1996.

1264 Neeb, P., Sauer, F., Horie, O., and Moortgat, G. K. Formation of hydroxymethyl hydroperoxide and formic acid
1265 in alkene ozonolysis in the presence of water vapour, *Atmos. Environ.*, 31, 1417–1423, 1997.

1266 Newland, M. J., Rickard, A. R., Alam, M. S., Vereecken, L., Muñoz, A., Ródenas, M., and Bloss, W. J.: Kinetics of stabilised
1267 Criegee intermediates derived from alkene ozonolysis: reactions with SO₂, H₂O and decomposition under boundary layer
1268 conditions, *Phys. Chem. Chem. Phys.*, 17, 4076-4088, 2015.

1269 Newland, M. J., Rickard, A. R., Sherwen, T., Evans, M. J., Vereecken, L., Muñoz, A., Ródenas, M., and Bloss, W. J.: The
1270 atmospheric impacts of monoterpene ozonolysis on global stabilised Criegee intermediate budgets and SO₂ oxidation:
1271 experiment, theory and modelling, *Atmos. Chem. Phys.*, 18, 6095-6120, 2018.

1272 Newland, M. J., Nelson B. S., Muñoz, A., Ródenas, M., Vera, T., Tarrega, J., and Rickard, A. R.: Trends in stabilisation of
1273 Criegee intermediates from alkene ozonolysis, *Phys. Chem. Chem. Phys.*, 22, 13698-13706, 2020.

1274 Nguyen, T. L., Winterhalter, R., Moortgat, G., Kanawati, B., Peeters, J., and Vereecken, L.: The gas-phase ozonolysis of β-
1275 caryophyllene (C₁₅H₂₄). Part II: A theoretical study, *Phys. Chem. Chem. Phys.*, 11, 4173-4183, 2009a.

1276 Nguyen, T. L., Peeters, J., and Vereecken, L.: Theoretical study of the gas-phase ozonolysis of β-pinene (C₁₀H₁₆), *Phys. Chem.
1277 Chem. Phys.*, 11, 5643-5656, 2009b.

1278 Nguyen, T. L., Lee, H., Matthews, D. A., McCarthy, M. C., and Stanton, J. F.: Stabilization of the Simplest Criegee
1279 Intermediate from the Reaction between Ozone and Ethylene: A High-Level Quantum Chemical and Kinetic Analysis of
1280 Ozonolysis, *J. Phys. Chem. A*, 119, 5524-5533, 2015.

1281 Nguyen, T. B., Tyndall, G. S., Crounse, J. D., Teng, A. P., Bates, K. H., Schwantes, R. H., Coggon, M. M., Zhang, L., Feiner,
1282 P., and Miller, D. O.: Atmospheric fates of Criegee intermediates in the ozonolysis of isoprene, *Phys. Chem. Chem. Phys.*, 18,
1283 10241-10254, 2016.

1284 Niki, H., Maker, P. D., Savage, C. M., Breitenbach, L. P., and Hurley, M. D. FTIR spectroscopic study of the mechanism for
1285 the gas-phase reaction between ozone and tetramethylethylene, *J. Phys. Chem. A*, 91, 941-946, 1987.

1286 O'Dwyer, M. A., Carey, T. J., Healy, R. M., Wenger, J. C., Picquet-Varrault, B., and Doussin, J. F.: The Gas-phase Ozonolysis
1287 of 1-Penten-3-ol, (Z)-2-Penten-1-ol, and 1-Penten-3-one: Kinetics, Products and Secondary Organic Aerosol Formation, *Z.
1288 Phys. Chem.*, 224, 1059-1080, 2010.

1289 O'Neal, H. E., and Blumstein, C.: A new mechanism for gas phase ozone-olefin reactions, *Int. J. Chem. Kinet.*, 5, 397-413,
1290 1973.

1291 Olzmann, M., Kraka, E., Cremer, D., Gutbrod, R., and Anderson, S.: Energetics, Kinetics, and Product Distributions of the
1292 Reactions of Ozone with Ethene and 2,3-Dimethyl-2-butene, *J. Phys. Chem. A*, 101, 9421-9429, 1997.

1293 Orzechowska, G. E., and Paulson, S. E.: Production of OH radicals from the reactions of C₄-C₆ internal alkenes and styrenes
1294 with ozone in the gas phase, *Atmos. Environ.*, 36, 571-581, 2002.

1295 Ouyang, B., McLeod, M. W., Jones, R. L., and Bloss, W. J.: NO₃ radical production from the reaction between the Criegee
1296 intermediate CH₂OO and NO₂, *Phys. Chem. Chem. Phys.*, 15, 17070-17075, 2013.

1297 Paulson, S. E., and Orlando, J. J. The reactions of ozone with alkenes: An important source of HO_x in the boundary layer,
1298 *Geophys. Res. Letts.*, 23, 3727-3730, 1996.

1299 Peltola, J., Seal, P., Inkilä, A., and Eskola, A.: Time-resolved, broadband UV-absorption spectrometry measurements of
1300 Criegee intermediate kinetics using a new photolytic precursor: unimolecular decomposition of CH₂OO and its reaction with
1301 formic acid, *Phys. Chem. Chem. Phys.*, 22, 11797-11808, 2020.

1302 Percival, C. J., Welz, O., Eskola, A. J., Savee, J. D., Osborn, D. L., Topping, D. O., Lowe, D., Utembe, S. R., Bacak, A.,
1303 McFiggans, G., Cooke, M. C., Xiao, P., Archibald, A. T., Jenkin, M. E., Derwent, R. G., Riipinen, I., Mok, D. W. K., Lee, E.
1304 P. F., Dyke, J. M., Taatjes, C. A., and Shallcross, D. E.: Regional and global impacts of Criegee intermediates on atmospheric
1305 sulphuric acid concentrations and first steps of aerosol formation, *Faraday Discuss.*, 165, 45-
1306 73, <https://doi.org/10.1039/C3FD00048F>, 2013.

1307 Pfeifle, M., Ma, Y. -T., Jasper, A. W., Harding, L. B., Hase, W. L., and Klippenstein, S. J.: Nascent energy distribution of the
1308 Criegee intermediate CH₂OO from direct dynamics calculations of primary ozonide dissociation, *J. Chem. Phys.*, 148, 174306,
1309 2018.

1310 Picquet-Varrault, B., Scarfogliero, M., and Doussin, J.-F.: Atmospheric Reactivity of Vinyl Acetate: Kinetic and Mechanistic
1311 Study of Its Gas-Phase Oxidation by OH, O₃, and NO₃, *Environ. Sci. Technol.*, **44**, 4615–4621, 2010.

1312 Pierce, J. R., Evans, M. J., Scott, C. E., D'Andrea, S. D., Farmer, D. K., Swietlicki, E., and Spracklen, D. V.: Weak global
1313 sensitivity of cloud condensation nuclei and the aerosol indirect effect to Criegee + SO₂ chemistry, *Atmos. Chem. Phys.*, **13**,
1314 3163–3176, <https://doi.org/10.5194/acp-13-3163-2013>, 2013.

1315 Pinelo, L., Gudmundsdottir, A. D., and Ault, B. S.: Matrix Isolation Study of the Ozonolysis of 1,3- and 1,4-Cyclohexadiene:
1316 Identification of Novel Reaction Pathways, *J. Phys. Chem. A*, **117**, 4174–4182, 2013.

1317 Raghunath, P., Lee, Y.-P., Lin, M. C.: Computational chemical kinetics for the reaction of Criegee intermediate CH₂OO with
1318 HNO₃ and its catalytic conversion to OH and HCO, *J. Phys. Chem. A*, **121**, 3871–3878, 2017.

1319 Rathman, W. C. D., Claxton, T. A., Rickard, A. R., Marston, G. A theoretical investigation of OH formation in the gas-phase
1320 ozonolysis of *E*-but-2-ene and *Z*-but-2-ene, *Phys. Chem. Chem. Phys.*, **1**, 3981–3985, 1999.

1321 Reissell, A., Harry, C., Aschmann, S. M., Atkinson, R., and Arey, J.: Formation of acetone from the OH radical- and O₃-
1322 initiated reactions of a series of monoterpenes, *J. Geophys. Res.*, **104**, 13869–13879, 1999.

1323 Rickard, A. R., Johnson, D., McGill, C. D., and Marston, G. OH Yields in the Gas-Phase reactions of Ozone with Alkenes, *J.*
1324 *Phys. Chem. A*, **103**, 7656–7664, 1999.

1325 Sakamoto, Y., Inomata, S., and Hirokawa, J.: Oligomerization Reaction of the Criegee Intermediate Leads to Secondary
1326 Organic Aerosol Formation in Ethylene Ozonolysis, *J. Phys. Chem. A*, **117**, 12912–12921, 2013.

1327 Saunders, S. M., Jenkin, M. E., Derwent, R. G., and Pilling, M. J.: Protocol for the development of the Master Chemical
1328 Mechanism, MCM v3 (Part A): Tropospheric degradation of non-aromatic volatile organic compounds, *Atmos. Chem. Phys.*,
1329 **3**, 161–180, 2003.

1330 Sheps, L., Scully, A. M., and: UV absorption probing of the conformer-dependent reactivity of a Criegee intermediate
1331 CH₃CHOO *Phys. Chem. Chem. Phys.*, **16**, 26701–26706, 2014.

1332 Sheps, L., Rotavera, B., Eskola, A. J., Osborn, D. L., Taatjes, C., Au, K., Shallcross, D. E., Khan, M. A. H., Percival, C. J.
1333 The reaction of Criegee intermediate CH₂OO with water dimer: Primary products and atmospheric impact, *Phys. Chem. Chem.*
1334 *Phys.*, **19**, 21970–21979, 2017.

1335 Sipilä, M., Jokinen, T., Berndt, T., Richters, S., Makkonen, R., Donahue, N. M., Mauldin III, R. L., Kurtén, T., Paasonen, P.,
1336 Sarnela, N., Ehn, M., Junninen, H., Rissanen, M. P., Thornton, J., Stratmann, F., Herrmann, H., Worsnop, D. R., Kulmala, M.,
1337 Kerminen, V.-M., and Petäjä, T.: Reactivity of stabilized Criegee intermediates (sCIs) from isoprene and monoterpene
1338 ozonolysis toward SO₂ and organic acids, *Atmos. Chem. Phys.*, **14**, 12143–12153, 2014.

1339 Smith, M. C., Chao, W., Takahashi, K., Boering, K. A., and Lin, J. J.-M.: Unimolecular Decomposition Rate of the Criegee
1340 Intermediate (CH₃)₂COO Measured Directly with UV Absorption Spectroscopy, *J. Phys. Chem. A*, doi:
1341 10.1021/acs.jpca.5b12124, 2016.

1342 Stephenson, T. A., and Lester, M. I.: Unimolecular decay dynamics of Criegee intermediates: Energy-resolved rates, thermal
1343 rates, and their atmospheric impact, *Int. Rev. Phys. Chem.*, **39**, 1–33, 2020.

1344 Stone, D., Blitz, M., Daubney, L., Howes, N. U. M., and Seakins, P.: Kinetics of CH₂OO reactions with SO₂, NO₂, NO, H₂O,
1345 and CH₃CHO as a function of pressure, *Phys. Chem. Chem. Phys.*, **16**, 1139–1149, 2014.

1346 Stone, D., Au, K., Sime, S., Medeiros, D. J., Blitz, M., Seakins, P., Decker, Z., and Sheps, L.: Unimolecular decomposition
1347 kinetics of the stabilised Criegee intermediates CH₂OO and CD₂OO, *Phys. Chem. Chem. Phys.*, **20**, 24940–24954, 2018.

1348 Taatjes, C. A., Welz, O., Eskola, A. J., Savee, J. D., Scheer, A. M., Shallcross, D. E., Rotavera, B., Lee, E. P. F., Dyke, J. M.,
1349 Mok, D. K. W., Osborn, D. L., and Percival, C. J.: Direct Measurements of Conformer-Dependent Reactivity of the Criegee
1350 Intermediate CH₃CHOO, *Science*, **340**, 177–180, 2013.

1351 [Taatjes, C. A., Caravan, R. L., Winiberg, F. A. F., Zuraski, K., Au, K., Sheps, L., Osborn, D. L., Vereecken, L., and Percival,](https://doi.org/10.1080/00268976.2021.1975199)
1352 [C. J.: Insertion products in the reaction of carbonyl oxide Criegee intermediates with acids: Chloro\(hydroperoxy\)methane](https://doi.org/10.1080/00268976.2021.1975199)
1353 [formation from reaction of CH₂OO with HCl and DCl, *Mol. Phys.*, **119**, e1975199,](https://doi.org/10.1080/00268976.2021.1975199)
1354 [https://doi.org/10.1080/00268976.2021.1975199, 2021.](https://doi.org/10.1080/00268976.2021.1975199)

1355 Tadayan S. V., Foreman, E. S., and Murray, C.: Kinetics of the reactions between the Criegee intermediate CH₂OO and
1356 alcohols, *J. Phys. Chem. A*, 122, 258-268, 2018.

1357 Thiault, G., Thévenet, R., Mellouki, A., and Le Bras, G.: OH and O₃-initiated oxidation of ethyl vinyl ether, *Phys. Chem.*
1358 *Chem. Phys.*, 4, 613-619, 2002.

1359 Tuazon, E. C., Aschmann, S. M., Arey, J., and Atkinson, R.: Products of the Gas-Phase Reactions of O₃ with a Series of
1360 Methyl-Substituted Ethenes, *Environ. Sci. Technol.*, 31, 10, 3004-3009, 1997.

1361 Vansco, M. F., Caravan, R. L., Zuraski, K., Winiberg, F. A. F., Au, K., Trongsirawat, N., Walsh, P. J., Osborn, D. L. Percival,
1362 C. J., Khan, M. A. H., Shallcross, D. E., Taatjes, C. A., and Lester, M. I.: Experimental Evidence of Dioxole Unimolecular
1363 Decay Pathway for Isoprene-Derived Criegee Intermediates, *J. Phys. Chem. A*, 124, 3542-3554, 2020.

1364 Vereecken, L., and Francisco, J. S.: Theoretical studies of atmospheric reaction mechanisms in the troposphere, *Chem. Soc.*
1365 *Rev.*, 41, 6259-6293, 2012.

1366 Vereecken, L., Novelli, A., and Taraborrelli, D.: Unimolecular decay strongly limits the atmospheric impact of Criegee
1367 intermediates, *Phys. Chem. Chem. Phys.*, 19, 31599-31612, 2017.

1368 Vereecken, L.: The reaction of Criegee intermediates with acids and enols, *Phys. Chem. Chem. Phys.*, 19, 28630-28640, 2017.

1369 Vereecken, L., and Nguyen, H. M. T.: Theoretical Study of the Reaction of Carbonyl Oxide with Nitrogen Dioxide: CH₂OO
1370 + NO₂, *Int. J. Chem. Kinet.*, 49, 752-760, 2017.

1371 Vereecken, L., Aumont, B., Barnes, I., Bozzelli, J., Goldman, M., Green, W., Madronich, S., McGillen, M., Mellouki, A.,
1372 Orlando, J., Picquet-Varrault, B., Rickard, A., Stockwell, W., Wallington, T., and Carter, W.: Perspective on Mechanism
1373 Development and Structure-Activity Relationships for Gas-Phase Atmospheric Chemistry. *Int. J. Chem. Kinet.*, 50, 435-469,
1374 <https://doi-org.insu.bib.cnrs.fr/10.1002/kin.21172>, 2018.

1375 Vichiatti, R. M., Keidel Spada, R. F., Ferreira da Silva, A. B., Correto Machado, F. B., and Andrade Haiduke, R. L.: Accurate
1376 Calculations of Rate Constants for the Forward and Reverse H₂O + CO ↔ HCOOH Reactions, *Chemistry Select*, 2, 7267-
1377 7272, 2017.

1378 Viero, L.: Kinetics and mechanisms for the oxidation of unsaturated organic acids and esters under atmospheric conditions,
1379 Ph.D. Thesis, University College Dublin, 2008.

1380 Wadt, W. R., and Goddard, W. A.: The electronic structure of the Criegee intermediate. Ramifications for the mechanism of
1381 ozonolysis, *J. Am. Chem. Soc.*, 97, 3004-3021, 1975.

1382 Wang, J., Zhou, L., Wang, W., and Ge, M.: Gas-phase reaction of two unsaturated ketones with atomic Cl and O₃: kinetics
1383 and products, *Phys. Chem. Chem. Phys.*, 17, 12000-12012, 2015.

1384 [Wang, S., Newland, M.J., Deng, W., Rickard, A.R., Hamilton, J.F., Muñoz, A., Ródenas, M., Vázquez, M.M., Wang, L. and](#)
1385 [Wang, X.: Aromatic photo-oxidation, a new source of atmospheric acidity, *Environmental Science & Technology*, 54, 7798-
1386 \[7806, 2020.\]\(#\)](#)

1387 Watson N. A. I., Black, J. A., Stonelake, T. M., Knowles, P. J., Beames, J. M.: An extended computational study of Criegee
1388 intermediate-alcohol reactions, *J. Phys. Chem. A*, 123, 218-229, 2019.

1389 Watson, N. A. I.: An Analysis of the Sources and Sinks for Criegee Intermediates: An Extended Computational Study, Ph.D.
1390 Thesis, University of Cardiff, <http://orca.cardiff.ac.uk/id/eprint/144742>, October 2021.

1391 Weidman, J. D., Allen, R. T., Moore, K. B., and Schaefer, H. F.: High-level theoretical characterization of the vinoxy radical
1392 ($\dot{\text{C}}\text{H}_2\text{CHO}$) + O₂ reaction. *J. Chem. Phys.*, 148, 184308, 2018.

1393 Welz, O., Savee, J. D., Osborn, D. L., Vasu, S. S., Percival, C. J., Shallcross, D. E., and Taatjes, C. A.: Direct Kinetic
1394 Measurements of Criegee Intermediate (CH₂OO) Formed by Reaction of CH₂I with O₂, *Science*, 335, 204-207, 2012.

1395 Welz, O., Eskola, A. J., Sheps, L., Rotavera, B., Savee, J. D., Scheer, A. M., Osborn, D. L., Lowe, D., Murray Booth, A., Xiao,
1396 P., Anwar H., Khan, M., Percival, C. J., Shallcross, D. E., and Taatjes, C. A.: Rate coefficients of C1 and C2 Criegee
1397 intermediate reactions with formic and acetic acid near the collision limit: direct kinetics measurements and atmospheric
1398 implications, *Angew. Chem. Int. Ed. Engl.*, 53, 4547-4750, 2014.

1399 Winterhalter, R., Neeb, P., Grossmann, D., Kolloff, A., Horie, O. and Moortgat, G.: Products and mechanism of the gas phase
1400 reaction of ozone with β -pinene. *Journal of Atmospheric Chemistry*, 35(2), 165-197, 2000.

1401 Winterhalter, R., Herrmann, F., Kanawati, B., Nguyen, T. L., Peeters, J., Vereecken, L., and Moortgat, G.: The gas-phase
1402 ozonolysis of β -caryophyllene ($C_{15}H_{24}$). Part I: an experimental study, *Phys. Chem. Chem. Phys.*, 11, 4152-4172, 2009.

1403 Wennberg, P. O., Bates, K. H., Crounse, J. D., Dodson, L. G., McVay, R. C., Mertens, L. A., Nguyen, T. B., Pranske, E.,
1404 Schwantes, R. H., and Smarte, M. D.: Gas-phase reactions of isoprene and its major oxidation products, *Chem. Rev.*, 118,
1405 3337–3390, <https://doi.org/10.1021/acs.chemrev.7b00439>, 2018.

1406 Wolff, S., Boddenberg, A., Thamm, J., Turner, W. V., and Gräß, S. Gas-phase ozonolysis of ethene in the presence of carbonyl-
1407 oxide scavengers, *Atmos. Environ*, 31, 2965-2969, 1997.

1408 Yu, J. Z., Cocker, D. R., Griffin, R. J., Flagan, R. C., and Seinfeld, J. H.: Gas-phase ozone oxidation of monoterpenes: Gaseous
1409 and particulate products, *J. Atmos. Chem.*, 34, 207–258, 1999.

1410 Zhao, Y., Wingen, L. M., Perraud, V., Greaves, J., and Finlayson-Pitts, B. J.: Role of the reaction of stabilized Criegee
1411 intermediates with peroxy radicals in particle formation and growth in air, *Phys. Chem. Chem. Phys.*, 17, 12500–12514, 2015.

1412 Zhou, S., Barnes, I., Zhu, T., Klotz, B., Albu, M., Bejan, I., and Benter, T.: Product Study of the OH, NO₃, and O₃ Initiated
1413 Atmospheric Photooxidation of Propyl Vinyl Ether, *Environ. Sci., Technol.*, 2006.

1414 Zhou, S.: Atmospheric Oxidation of Vinyl Ethers, PhD thesis, Bergische Universität Wuppertal, 2007.

1415 Ziemann, P. J.: Evidence for Low-Volatility Diacyl Peroxides as a Nucleating Agent and Major Component of Aerosol Formed
1416 from Reactions of O₃ with Cyclohexene and Homologous Compounds, *J. Phys. Chem. A*, 106, 4390–4402, 2002.

1417